SPLICING REPRESSION IS A MAJOR FUNCTION OF TDP-43 IN MOTOR NEURONS: THERAPEUTIC IMPLICATIONS FOR AMYOTROPHIC LATERAL SCLEROSIS

by

Aneesh N. Donde

A thesis submitted to Johns Hopkins University in conformity with

the requirements for the degree of Doctor of Philosophy

Baltimore, Maryland
May, 2018

Title: Splicing Repression is a Major Function of Tdp-43 in Motor Neurons

Ph.D Dissertator: Aneesh N. Donde

Ph.D Advisor: Philip C. Wong, Ph.D

Abstract

Nuclear depletion of TDP-43, an RNA binding protein which serves to protect the transcriptome by repressing aberrant splicing, may underlie neurodegeneration in amyotrophic lateral sclerosis (ALS). As multiple functions have been ascribed to TDP-43, whether splicing repression is its major role in motor neurons – that may be compromised in ALS – remains to be established. Here, we show that TDP-43 mediated splicing repression is central to the physiology of motor neurons. To validate TDP-43 mediated splicing repression as a therapeutic target, an AAV9-mediated gene delivery approach was employed to deliver a chimeric protein comprised of the N-terminal RNA recognition domain of TDP-43 fused to an unrelated splicing repressor (RAVER1) to mice lacking TDP-43 in motor neurons. This strategy allowed long-term expression of the repressor without any untoward effects, delayed the onset and slowed the progression of disease, and extended survival. In treated mice, evidence of aberrant splicing was markedly decreased and accompanied by amelioration of motor neuron loss. These findings establish that splicing repression is a principal role of TDP-43 in motor neurons and support the idea that loss of TDP-43-mediated splicing repression represents a key pathogenic mechanism underling motor neuron loss, validating a novel mechanism-based therapeutic strategy for ALS.

Dissertation Committee:

Philip C. Wong, Ph.D.

Charlotte J. Sumner, M.D.

Lee Martin, Ph.D.

Tom Lloyd, M.D., Ph.D.

Acknowledgements

First and foremost, I would like to thank Philip Wong for being an exceptional mentor and thesis advisor to me during my tenure at Johns Hopkins. His unwavering support and guidance has carried me through the difficult times, and I am extremely grateful for the opportunity to work with and learn from him. As my role model, Phil has played an instrumental role in shaping me in becoming the scientist and person that I am today, and one day, I hope to be like him and pass on the same lessons he has taught me.

I would also like to thank the members of my thesis committee: Charlotte Sumner, Lee Martin, and Tom Lloyd, for their thoughtful and insightful discussions and comments regarding my thesis project. I appreciate all the input they have provided during my thesis meetings and individual discussions. I would also like to thank Liam Chen for collaborating with me on several projects and providing me the opportunity to write a review article on gene therapy in CNS neurodegenerative disease.

The departments of Neuroscience and Pathology at Johns Hopkins have provided invaluable resources that have made my thesis project possible, and for that, I am deeply grateful. In particular, I would like to thank Rita Ragan and Beth Wood-Roig of the Neuroscience department, and Elaine Delman, Argie Laffoon, and Sherry Reed of the Pathology department for their administrative assistance.

Lastly, I would like to thank the current and past members of my lab, my friends in the graduate program, and my family for their unwavering support and companionship during my journey.

Table of Contents

List of Figures and Tables:

Chapter 1: Introduction

Introduction

Amyotrophic lateral sclerosis (ALS), also known as Lou Gehrig's disease, is the most common motor neuron disease (Table 1) characterized by the death of upper and lower motor neurons*(Cleveland, Rothstein, Cleveland, & Rothstein, 2001; del Aguila, Jr, McGuire, Koepsell, & van Belle, 2003)*. Patients with ALS show progressively worsening weakness, spasticity, muscle atrophy, and an eventual loss of voluntary muscle control*(Cleveland et al., 2001; del Aguila et al., 2003)*. With an incidence rate of 2 per 100,000 people, the average life expectancy following diagnosis of this incurable disease is only 2-5 years, with most deaths occurring due to respiratory failure*(Cleveland et al., 2001; del Aguila et al., 2003; Julien, 2001)*. The genetic underpinnings of ALS are complex, with only about 5-10% of ALS cases showing a recognizable family history of disease, termed 'familial' ALS (fALS), and the remaining 90-95% of cases termed 'sporadic' ALS (sALS). While the pathophysiology of ALS was described by Jean-Martin Charcot in 1874, to this day, the molecular mechanisms underlying motor neuron death in ALS still remain unknown. Nevertheless, important work over the last several decades has provided valuable insights into the causes and progression of this currently incurable disease.

In 1993, it was discovered that mutations in the Cu-Zn superoxide dismutase (SOD1) gene were associated with ~20% of fALS, representing ~2% of all ALS cases*(Jones, Brock, Chancellor, Warlow, & Swingler, 1993; Rosen et al., 1993)*. While the exact mechanisms through which mutant SOD1 affects motor neuron health are not fully elucidated to this day, this discovery allowed for the generation of the first transgenic mouse models ($SOD1^{G93A}$ mice), allowing researchers new opportunities to explore disease mechanisms and potential treatment options in a vertebrate model system. In the following years, mutations in several

other genes, such as ALS2, OPTN, VCP, TBK1, and UBQLN, among others, were associated with ALS and consequently have also been studied in animal models (Table 2). However, as these genetic mutations, taken together, only represent a small fraction of total ALS patients, our understanding of the molecular underpinnings of most cases of ALS still remained minimal. Furthermore, many of these genes affected diverse pathways and cellular functions, complicating efforts at identifying a unifying downstream mechanism of motor neuron death in ALS that could be targeted for therapeutic intervention.

One major breakthrough in the ALS field was made in 2006, when it was discovered that in neurons and oligodendrocytes of patients with sALS, Tar DNA-binding protein 43 (TDP-43, encoded by the gene *TARDBP*), an essential, highly-conserved RNA binding protein*(Sephton et al., 2010; L. S. Wu et al., 2010)*, unusually depletes from the nucleus and aggregates in ubiquitinated cytoplasmic inclusions*(Neumann et al., 2006)*. These TDP-43 positive inclusions were visible in ~95% of patients with sALS and ~50% of patients with frontotemporal dementia (FTD), the second most common type of young-onset dementia with an incidence rate of 10-30 per 100,000 people*(Arai et al., 2006a; Sieben et al., 2012)*. Two important implications could be drawn from this finding. Firstly, this observation, coupled with clinical evidence of symptom overlap between ALS and FTD*(Lomen-Hoerth, Anderson, & Miller, 2002)*, has led to the idea that these two diseases exist on a spectrum (termed ALS/FTD). Secondly, the fact that TDP-43 mislocalization could be observed in a vast majority of total ALS cases suggested that this protein plays a fundamental role in disease. Supporting this claim was the subsequent discovery that missense mutations in TDP-43, which mostly cluster within its C-terminal domain, are linked to familial ALS*(Kabashi et al., 2008; Sreedharan et al., 2008)*. Additionally, various other

genetic mutations associated with familial ALS/FTD, such as UBQLN, ATXN2, SQSTM1, and TBK1 are associated with TDP-43 pathology (Table 2). Of particular note is the observation that TDP-43 mislocalization is observed in patients carrying a hexanucleotide repeat expansion in *C9ORF72*, recently discovered to be the most common genetic cause of ALS/FTD*(Chew et al., 2015)*. Furthermore,TDP-43 pathology is evident in a subset of patients with inclusion body myositis (IBM) *(Salajegheh et al., 2009)* and Alzheimer's disease (AD) *(Amador-Ortiz et al., 2007; Josephs et al., 2014)*. TDP-43 pathology is notably absent in neurons of patients with SOD1 mutations*(Mackenzie et al., 2007)*, suggesting that motor neuron death may occur through distinct mechanisms in SOD1-ALS and potentially necessitating the division of ALS/FTD into different sub-types. Nevertheless, these observations support the notion that in the vast majority of ALS/FTD cases, TDP-43 mislocalization is central to disease pathogenesis and presents a final common pathogenic pathway.

Gain and Loss of Function Models of TDP-43 Pathology

To date, the precise mechanism underlying TDP-43 pathology in ALS/FTD remains unclear, as loss of nuclear function, cytoplasmic toxic gain of function, or both, may contribute to disease. Animal studies have provided some insight into this problem. Initial efforts focused on studies of transgenic wild-type human and ALS-linked mutant human TDP-43 overexpression models*(Ash et al., 2010; Shan, Chiang, Price, & Wong, 2010; Wils et al., 2010; Xu et al., 2010)*. Overexpression of both wild-type and mutant TDP-43 in multiple model systems results in age-dependent neurodegeneration and behavioral deficits consistent with the phenotype of ALS/FTD. However, transgenic overexpression does not always recapitulate important

pathological features of ALS, such as cytoplasmic aggregation. Furthermore, as TDP-43 binds to its own 3' untranslated region (UTR) to tightly autoregulate its own transcript levels, transgenic mutant TDP-43 overexpression can suppress endogenous mouse Tdp-43*(Winton et al., 2008)*. Recent research demonstrated that transgenic cytoplasmic accumulation of mutant TDP-43 with a nonfunctional nuclear localization sequence (NLS) in neurons of mice resulted in depletion of endogenous nuclear Tdp-43, raising the question as to whether the observed neurodegenerative phenotype was due to cytoplasmic accumulation or nuclear loss of TDP-43*(Spiller et al., 2016)*. Hence, the precise contribution of toxic gain of function of TDP-43 has remained unclear.

Subsequent research has suggested that depletion of nuclear TDP-43 plays a critical role in motor neuron degeneration as well. While global knockout of TDP-43 is embryonically lethal*(Kraemer et al., 2010)*, our lab and others have demonstrated that post developmental tissue-specific deletion of TDP-43 also recapitulates the age-dependent progressive neurodegeneration of ALS/FTD*(Feiguin et al., 2009; Kraemer et al., 2010; Schmid et al., 2013; Vanden Broeck, Callaerts, & Dermaut, 2014; C. Yang, Wang, Qiao, Yang, Aliaga, Qiu, Tan, Salameh, McKenna-Yasek, Smith, Peng, Moore, Brown, Cai, & Xu, 2014a; Zuo-Shang Xu, 2012)*. Interestingly, Vatsavayai and colleagues reported nuclear clearance of TDP-43 – but not cytoplasmic TDP-43 aggregates – in a brain biopsy of a patient five years prior to their first symptoms of FTD*(Vatsavayai et al., 2016a)*. Brain tissue examined at autopsy, 8 years after symptom onset, did contain cytoplasmic TDP-43 inclusions, suggesting that nuclear loss of TDP-43 may represent an earlier event in disease pathogenesis, potentially even preceding the

onset of clinical symptoms. Therefore, research exploring the contribution of loss of nuclear TDP-43 function to neuronal survival is of critical importance.

Recent work has uncovered evidence of impaired nucleocytoplasmic trafficking in several neurodegenerative diseases, including ALS/FTD*(K. Zhang et al., 2015)*. The interplay between nucleocytoplasmic transport, cytoplasmic TDP-43 accumulation, and nuclear depletion of TDP-43 is complex; while TDP-43 mislocalization may be a downstream consequence of defective nucleocytoplasmic transport, newer evidence suggests that cytoplasmic aggregation of TDP-43 itself impairs the nuclear pore complex and nucleocytoplasmic transport*(Chou et al., 2018)*. Ultimately, both toxic gain of function and loss of function of TDP-43 are thought to play important roles in disease.

TDP-43 Represses Aberrant Splicing

In order to better understand the contribution of pathological TDP-43 mislocalization to disease, one important step is to better understand the essential function(s) of this protein in neurons. TDP-43 is thought to play important roles in several essential cellular processes in both the nucleus and cytoplasm, including cellular stress response pathways*(McDonald et al., 2011)*, mRNA delivery to dendritic or axonal compartments*(Alami et al., 2014)*, or phase separation of membrane-less organelles*(Gopal, Nirschl, Klinman, & Holzbaur, 2017; Molliex et al., 2015)*. As a member of the heterogenous ribonuclear protein (hnRNP) family, TDP-43 is concentrated in transcriptionally active euchromatin regions*(Casafont, Bengoechea, Tapia, Berciano, & Lafarga, 2009)*, and is thought to regulate alternative splicing*(Buratti et al., 2001; Polymenidou et al., 2011; Prudencio et al., 2015; Tollervey et al., 2011)*. TDP-43 interacts with

many proteins and RNAs, potentially regulating numerous pathways and complicating efforts at developing mechanism-based therapies*(Fiesel et al., 2010; Freibaum, Chitta, High, & Taylor, 2010)*.

Recently, our lab discovered that TDP-43 is the founding member of a class of proteins that act as a guardian of the transcriptome by repressing aberrant splicing *(Ling, Pletnikova, Troncoso, & Wong, 2015)*, a function that is compromised in cases of neurodegenerative diseases with TDP-43 pathology*(Jeong et al., 2017; Sun et al., 2017a)*. Depletion of TDP-43 leads to expression of transcripts with abnormal incorporation of aberrant 'cryptic' exons in UG-rich, normally intronic regions. Advancements in the resolution of RNA-sequencing technologies have only recently allowed for transcriptomic analysis to uncover these previously elusive splicing changes. Evidence of cryptic exon incorporation can be observed in cases of ALS/FTD, IBM, and AD displaying TDP-43 pathology, providing a useful biomarker for loss of nuclear TDP-43 function and suggesting that loss of this splicing repression function may underlie disease pathogenesis*(Jeong et al., 2017; LaClair et al., 2016; Sun et al., 2017b)*.

Subsequent analysis of the cryptic exon profile in different cell types revealed that due to the non-conserved nature of the UG-rich intronic regions, the exact transcripts affected by loss of TDP-43 function are highly variable between organisms and cell types; hence, TDP-43 loss may impair cell type-specific pathways in unique ways*(Jeong et al., 2017)*. However, impaired splicing repression, leading to the loss of transcriptional fidelity, may represent a common, upstream cause of neuronal death in ALS/FTD. While the exact targets affected by compromised splicing repression in TDP-43 knockout tissues is variable, the splicing repression function of TDP-43 is highly conserved across species, suggesting that a therapeutic strategy

that restores TDP-43's function may be more viable than one aimed at restoring any one particular transcript*(Jeong et al., 2017)*. Since TDP-43 is involved in multiple other intracellular roles, however, it remains unknown whether splicing repression is a major function of TDP-43 in motor neurons. If so, restoring this function in affected motor neurons would represent a promising new mechanism-based therapeutic approach for ALS/FTD and potentially for other human diseases with TDP-43 pathology.

Using a mouse model system, we establish here that TDP-43-mediated splicing repression is central to the physiology of motor neurons. First, we confirm in two different mouse models that postnatal deletion of *Tdp-43* in either forebrain excitatory neurons or motor neurons results in progressive, age-dependent neurodegeneration. In tissues from both mouse models, we observe evidence of compromised splicing repression. Next, using an AAV9-mediated gene delivery approach*(Foust et al., 2010)*, we validate a mechanism-based therapeutic strategy to restore TDP-43-mediated splicing repression to attenuate neurodegeneration caused by the loss of nuclear TDP-43 function. These findings provide a potential molecular basis of TDP-43 pathology in motor neurons and establish a proof-of-principle for a rational, mechanism-based strategy for the treatment of ALS.

Chapter 2: Methods

Methods

Mouse Generation

All mouse procedures were performed in accordance with the National Institutes of Health Guide for the Care and Use of Laboratory Animals and were approved by the Johns Hopkins University Animal Care and Use Committee.

We crossbred our previously described conditional *Tardbp* knockout mice (Chiang et al, PNAS 2010) (*Tardbp*$^{F/F}$, Jax stock 017591) with ChAT-IRES-Cre transgenic mice on a C57BL/6J background (Jax stock 006410) to obtain a cohort of ChAT-IRES-Cre;*Tardbp*$^{F/+}$ mice. These were subsequently crossed again with *Tardbp*$^{F/F}$ mice to generate the final cohort of ChAT-IRES-Cre;*Tardbp*$^{F/+}$ (control) and ChAT-IRES-Cre;*Tardbp*$^{F/F}$ (Tdp-43 knockout) mice. All mice were housed under a 12L:12D daily cycle and managed by Johns Hopkins University Research Animal Resources (RAR).

We depleted TDP-43 in the forebrains of adult mice in a similar manner by crossing our *Tardbp*$^{F/F}$ mice to those CaMKIIa-Cre^{ER} mice to generate tamoxifen-inducible conditional *Tardbp* knockout mice (CaMKIIa-Cre^{ER};*Tardbp*$^{F/F}$ mice, termed cT) mice, allowing tamoxifen-induced recombination in excitatory forebrain neurons at maturity. Oral tamoxifen citrate was administered to all animals in the feed (Harlan Teklad) at an average 40 mg/kg/day for a 4week period beginning at p42-46, and mice were singly housed during this period to monitor tamoxifen-feed intake.

Viral Vector Packaging

CTR was cloned as previously described*(Ling et al., 2015)*. AAV9 packaging was performed by Virovek (Hayward CA), and CTR or GFP expression was independently confirmed by HeLa cell transduction and western blot prior to all experiments.

Intracerebroventricular (ICV) Injection

All injections were performed on mouse pups within 8 hours of birth. Pups were cryo-anaesthetized on wet ice for no longer than 2 minutes. A latex barrier between pups and ice prevented skin damage. A sterile, single-use pulled glass needle (Drummond microcaps, 41 mm length, approx. 0.5 mm minimum diameter) was penetrated 3mm into the lateral ventricle of each cryo-anaesthetized mouse pup to slowly deliver 3 µl of AAV9 ($1E10^{13}$ vg/ml) carrying either our chimeric splicing repressor protein, termed CTR, or GFP into the lateral ventricles over 15 seconds; solutions contained 0.05% trypan blue dye for localization. Pups recovered under a heat lamp with bedding from their home cage in order to restore scent, after which they were returned to their mother cage and monitored after 6 and 12 hours and daily afterwards. A successful injection was identified by dye-induced darkening of the spinal column at 6 hours post-injection. Approximately 80% of pups successfully recovered from injection, with 10% insufficiently recovering from anesthesia at p0-p1 and 10% displaying signs of hydrocephaly at p14-p21. All pups showing signs of distress at any time following recovery were euthanized.

Sample Size

Sample sizes for all cohorts examined in the CTR rescue study are presented in Table 3. All litters were injected prior to genotyping. For motor function and survival analyses, a total of 40 mice from 8 litters were injected for cohort 1. Every pup in each litter was injected at random with an AAV9 vector carrying either our CTR fusion protein or GFP as a control, and all pups in

each litter received either CTR or GFP. A total of 8 ChAT-IRES-Cre;*Tardbp*$^{F/+}$ mice were injected with GFP, 8 ChAT-IRES-Cre;Tardbp$^{F/+}$ mice were injected with CTR, 11 ChAT-IRES-Cre;*Tardbp*$^{F/F}$ were injected with GFP, and 11 ChAT-IRES-Cre;*Tardbp*$^{F/F}$ mice were injected with CTR. The size of cohort 1 was sufficiently powered to measure a mean survival increase of 50% with 25% standard deviation (1-β = 0.994). We then replicated our results by injecting a second cohort of mice from the same breeder pairs, termed 'cohort 2'. Each litter in cohort 2 received the opposite payload as its cohort 1 counterpart. Two additional cohorts, each from the same breeder pairs, were bred and injected for analysis of spinal cord pathology at p90 (pathology analysis cohort) and for injection of an AAV9 vector carrying only the N-terminal fragment of TDP-43 as another control (N-terminal fragment cohort).

Hanging Wire Test

Hanging wire tests*(Deacon, 2013)* were performed weekly beginning at p30. Investigators were blinded to the treatment group of each animal. Each mouse was placed on the center of a metal grid that then was shaken gently to prompt the mouse to hold on before being turned upside down 30 cm over an empty cage. Each mouse was allowed up to three attempts to hold on to the inverted grid for an arbitrary maximum of 60 seconds. Mice were given >2 minutes of rest between attempts, and the best attempt was used for analyses.

Accelerating Rotarod Test

Rotarod tests*(Deacon, 2013)* were performed once every two weeks with an initial acclimatization session beginning at p30. Investigators were blinded to the treatment group of each animal. Mice were placed on the apparatus (Rotamex 5, Columbus Instruments) with a rod diameter of 3 cm, minimum speed of 4 rpm, and accelerating at&& 20 rpm/min. Latency to fall

was recorded. Each mouse was given three attempts with >30 minutes of rest between attempts, and the best attempt was used for analyses.

Elevated Plus Maze Test

The elevated plus maze (San Diego Instruments) test was performed to evaluate levels of anxiety-like behavior. This maze was made of stainless steel and consisted of two closed arms measuring 19.5 inches in length × 4 inches in width × 15.5 inches in height and two open arms measuring 19.5 inches in length × 4 inches in width. These arms were connected by a 4 × 4-inch platform. Each mouse was placed on the center platform and remained in the maze for 5 min. Number of visits and time spent in the closed arms and open arms was measured*(LaClair et al., 2016)*.

Spontaneous Alternation Y Maze Test

The Y-maze has three arms (18.5 inches in length × 2.5 inches in width × 1 inch in height) radiating at equal angles from a central platform. Mice were place into the end of one arm and allowed to explore freely for 5 min. The sequence of arm entries was recorded. The spontaneous alternation behavior was calculated as the number of triads containing entries into all three arms divided by the maximum possible alternations*(LaClair et al., 2016)*.

Survival

Upon showing symptoms of hindlimb paralysis, mice were provided wet chow and Dietgel on the cage floor. End-stage was defined as a failure of a mouse to right itself within 10 seconds when placed on its back on the cage floor and was tested daily after hindlimb paralysis was observed. Investigators were blinded to the treatment group of each animal. All mice were sacrificed and processed for biochemical and pathological analysis upon reaching end-stage.

RT-PCR

Total RNA was extracted from hippocampi of 3 month old female CamKIIa-Cre;*Tardbp*$^{F/F}$ (knockout) and littermate control mice (CamKIIa-Cre;*Tardbp*$^{F/+}$) using TRIzol (Life Tech.) and RNeasy Mini kits (Qiagen). Three control brains and three knockout brains were analyzed, and all mice were female. Total RNA was isolated using RNeasy Mini Kit (Qiagen). cDNA was synthetized using RevertAid First Strand cDNA Synthesis Kit (Thermo Scientific) with random primers. Primers used to amplify cryptic exons were as follows: Ap3b2 F: AGCCAGAATATGGCCACGAC; Ap3b2 R: CACTATGATGGGCACACGGA; Camk1G F: CTGGCCAAGATCACAGACTGG; CamK1G R: CTGTGTAGACACCACGCTCT.

Quantitative PCR

Whole spinal cords of p45 ChAT-IRES-Cre;*Tardbp*$^{F/+}$ and ChAT-IRES-Cre;*Tardbp*$^{F/F}$ mice were dissected, titurated using a 1 mL syringe with a 20-gauge needle, and placed in TRIzol. RNA from whole fly heads was extracted in a similar way. Total poly-A-containing messenger RNA was extracted using a RNeasy Mini kit (Qiagen) protocol under RNAse-free conditions and converted to cDNA using the Protoscript II First Strand cDNA Synthesis Kit (NEB). Quantitative PCR for cryptic exon mRNA was performed using the PowerUp SYBR Green protocol (Applied Biosystems) with the following primers: GGCT F: GAGGGGTGTTGGAAGGCTGT; GGCT R: TACCACTCCCCACACTTCGT; SYNJ2BP F: CTCCAACGACAGTGGCATCT; SYNJ2BP R: TCTTCCTGAGGACCTCCGTT; IFT81 F: AAGTGCGAGGACTTCGTGAG; IFT81 R: CAGCGATCTGTCTGCTTTGC; GAPDH F: AGGTCGGTGTGAACGGATTTG; GAPDH R: GGGGTCGTTGATGGCAACA; TBP F: AAGGGAGAATCATGGACCAG; TBP R: CCGTAAGGCATCATTGGACT. Each reaction was performed in duplicate, and each RT-PCR

experiment independently repeated three times. Relative transcript levels were calculated in Microsoft Excel according to the formula: (POWER(2, −(C_t mean *cryptic exon target*)))/(POWER(2, –(AVERAGE(C_t mean *TBP*, C_t mean *GAPDH*))).

Histological and Immunohistochemical Analysis

P90 mice from the pathology analysis cohort were anaesthetized and perfused with 4% paraformaldehyde. The cervical (C5-C8) and lumbar (L1-L3) enlargements and their corresponding spinal ganglions from each mouse were dissected and post-fixed for 24 hours. Spinal ganglions were embedded in epoxy resin and sagittally sectioned at 1 µm thickness. Spinal cords were embedded in paraffin and sagittally sectioned at 10 µm thickness. Sections were stained with hematoxylin/eosin or Cresyl violet for histological analysis.

For immunohistochemical analysis, sections were deparaffinized and incubated in 10 mM citric acid at 95 C for 10 minutes followed by a 30-minute incubation in 0.3% hydrogen peroxide in methanol to quench endogenous peroxidase activity. Normal goat serum (5%) in PBS-T was used to block nonspecific binding, after which primary antibody in blocking buffer was applied to each section overnight at 4 C in a humid chamber. Secondary antibodies were applied at room temperature for 2 hours. A Vectastain Universal Elite ABC kit (Vector Laboratories) was used to amplify signal.

Sections were stained with the following primary antibodies: Human-specific N-terminus TDP-43 (hTDP43, 1:500; AB57105, Abcam), Choline acetyltransferase (ChAT, 1:1000; AB144, Millipore), C-terminus TDP-43 (1:500; 12892-1AP, Proteintech), microtubule-associated protein 2 (Map2, 1:1,000; AB5622, Millipore), phosphorylated neurofilament (Smi31, 1:1,000; BioLegend), synaptophysin (1;1000; SY38/ab8049, Abcam), ionized calcium-binding adapter

molecule 1(IBA1, 1:500; 10904-1AP, Proteintech), glial fibrillary acidic protein (GFAP, 1:500; AB7260, Abcam), phosphorylated tau (Tau422, 1:1000; AB79415, Abcam).

Immunoblot Analysis

Whole spinal cords from p90 mice were flushed and homogenized using a 1 mL syringe with a 20-gauge needle in cold RIPA buffer with protease inhibitor cocktail (Roche). Protein concentration in the supernatants was determined via BCA assay (Pierce), and 10 µg protein was loaded on a 10% Bis-Tris SDS-PAGE gel (Novex) and transferred to a PVDF membrane, which was probed with the following antibodies: N-terminal TDP-43 (1:2000; 10782-2-AP, Proteintech), β-tubulin III (1:20,000; T2200, Sigma).

Data and Statistical Analysis

Histological and RNA data was analyzed using the unpaired, two-tailed Student's t-test with Tukey's multiple comparison where appropriate, and one-way analysis of variance (ANOVA) test using Stata 10 for Mac (Statacorp) and Graphpad Prism for Mac (Graphpad Software). Mouse hanging wire, rotarod, and weights were analyzed using two-way ANOVA with Tukey's multiple comparison. Kaplan-Meier survival curves were analyzed using the log-rank test. P values of < 0.05 were considered significant.

Chapter 3: Results

Results

Conditional Deletion of *Tdp-43* Results in Age-Dependent Neurodegeneration

As a first step, to determine whether cell type-specific conditional deletion of Tdp-43 can lead to age-dependent neurodegeneration, a major phenotype of ALS/FTD, we took advantage of our Tdp-43 conditional knockout mice, in which exon 3 of *Tdp-43* was flanked by loxp sites*(Chiang et al., 2010)* (*Tardbp*$^{F/F}$), and crossbred them with a choline acetyltransferase (ChAT) dependent Cre driver line*(Rossi et al., 2011)* (ChAT-IRES-Cre) to generate a line lacking Tdp-43 in >95% of ChAT-positive spinal motor neurons by p30 (ChAT-IRES-Cre;*Tardbp*$^{F/F}$ mice, Figure 1A). Homozygous cell type-specific knockout is necessary because global Tdp-43 deletion is embryonically lethal, and heterozygous knockout mice show normal levels of Tdp-43 due to autoregulation*(Chiang et al., 2010; Kraemer et al., 2010)*. Our Tdp-43 conditional knockout mice showed progressive, age-dependent loss of cervical and lumbar motor neurons and a reduction number and caliber of ventral, but not dorsal, root axons (Figures 2, 10, 11). ChAT-IRES-Cre;*Tardbp*$^{F/F}$ mice also exhibited reduced body weight and showed tremor, hindlimb weakness, and paralysis with mortality occurring around 8-10 months (Figures 8A, red line). This phenotype is consistent with other, previously reported motor neuron Tdp-43 knockout mouse models*(Iguchi et al., 2013; L. S. Wu, Cheng, & Shen, 2012; C. Yang, Wang, Qiao, Yang, Aliaga, Qiu, Tan, Salameh, McKenna-Yasek, Smith, Peng, Moore, Brown, Cai, & Xu, 2014b)*. As predicted, we found evidence of aberrant splicing and cryptic exon incorporation in the spinal cords of p45 ChAT-IRES-Cre;*Tardbp*$^{F/F}$ mice through quantitative RT-PCR (Figure 12, red bars).

As our ChAT-dependent Cre driver expresses before ~p30 (Figure 1B), we then wondered whether the observed phenotype in our motor neuron knockout mice truly reflects

age-dependent neurodegeneration, or is rather due to residual effects from motor neuron neurodevelopmental defects. Additionally, we wondered if Cre-mediated Tdp-43 excision from excitatory forebrain neurons could be used to model TDP-43 dysfunction in FTD or AD as well. To answer these questions, we took advantage of another driver line (CaMKIIa-Cre^{ER}) to generate CaMKIIa-Cre^{ER};*Tardbp*$^{F/F}$ mice (Figure 3A), in which tamoxifen-induced recombination at p42 resulted in depletion Tdp-43 in ~80% of post-developmental excitatory pyramidal neurons in the hippocampus and ~40% in the cortex (Figure 3B-D). Age-dependent loss of these forebrain neurons mimics observations of neuronal loss in patients with FTD or AD. Like our motor neuron Tdp-43 knockout mice, our forebrain knockout mice also showed progressive, age-dependent loss of cortical and hippocampal neurons, reduced brain volume, and worsening behavioral and cognitive abnormalities (Figures 4-5). RT-PCR analysis of hippocampal lysate from non-inducible p90 mice under the same promoter (CaMKIIa-Cre;*Tardbp*$^{F/F}$ mice) confirmed the incorporation of aberrant cryptic exons in knockout mice (Figure 6). Taken together, these results confirm that postnatal deletion of neuronal Tdp-43 in mice leads to age-dependent neurodegeneration, a major phenotype observed in ALS/FTD or AD.

A Chimeric Protein (CTR) Restores Splicing Repression in Mice lacking *Tardbp* in Motor Neurons

We previously found that TDP-43 maintains splicing fidelity by repressing previously unannotated 'cryptic' exons *(Ling et al., 2015)*. TDP-43 mediated splicing repression can be restored using a chimeric protein, termed CTR, consisting of the RNA-recognizing N-terminal domain of TDP-43 fused with an unrelated, structurally distinct but well characterized splicing

repressor, RAVER1 (Figure 7C)*(Gromak et al., 2003; Ling et al., 2015; Rideau et al., 2006)*. The C-terminal domain of TDP-43, a region that harbors most disease-causing mutations and contains a low-complexity prion-like domain thought to be potentially responsible for pathological cytoplasmic TDP-43 aggregation in ALS/FTD*(Conicella, Zerze, Mittal, & Fawzi, 2016)*, was replaced by the splicing repression domain from RAVER1, a region with no sequence similarity to TDP-43. Previous work in our lab has validated that the CTR fusion protein is able to enter the nucleus and repress splicing as predicted in a cell culture model*(Ling et al., 2015)*. However, since multiple roles have been ascribed to TDP-43*(Buratti et al., 2001; Casafont et al., 2009; Fiesel et al., 2010; Freibaum et al., 2010; Gendron, Josephs, & Petrucelli, 2010; Ling et al., 2015; Ou, Wu, Harrich, Garca-Martnez, & Gaynor, 1995)*, it is not known whether splicing repression is central to the physiology of mammalian motor neurons *in vivo*. To determine whether splicing repression is a major role of TDP-43 in motor neurons, we elected to use AAV9 to deliver CTR to central neurons of mice lacking TDP-43 in spinal motor neurons, a model which exhibits age dependent motor neuron disease accompanied by evidence of incorporation of TDP-43 cryptic exons (see above).

To deliver our fusion protein to motor neurons in mice, we selected adeno-associated virus serotype 9 (AAV9) as our vector due to its neuronal tropism in neonatal mice, minimal immunogenicity, and episomal persistence*(McMenamin & Wood, 2010; Weinberg, Samulski, & McCown, 2013)*. AAV technology has also been previously validated as safe and effective in human clinical trials, thereby improving the therapeutic relevance of our strategy*(Janson et al., 2002; Kaplitt et al., 1994)*. Intracerebroventricular (ICV) injections allowed us to effectively target motor neurons, as cerebrospinal fluid (CSF) flow allowed the virus to transduce cells

throughout the spinal cord. Neonatal (rather than adult) mice were treated for three reasons: Firstly, for poorly understood reasons, the neuronal tropism of AAV9 appears strongest in neonates*(Foust et al., 2009; Howard, Powers, Wang, & Harvey, 2008)*; secondly, by introducing the CTR protein at an early age, we hoped to maximize the observed rescue effect; lastly, using neonatal mice necessitated a minimal viral dose, thereby allowing us to increase our sample size for all experiments.

Perinatal unilateral intracerebroventricular injection of AAV9 ($3x10^{10}$ vg/mouse) carrying our CTR chimeric construct (Figure 7C) under a ubiquitous chicken beta-actin hybrid (CBhA) promoter selected for its robust long-term expression*(Kawamoto, Shi, Nitta, Miyazaki, & Allen, 2005)* resulted in CTR protein expression in 50-60% of cervical and lumbar motor neurons, first observed at p30 and persisting to at least 8 months in mice (Figure 7A). Transgenic expression was strongest in the nucleoplasm, with no evidence of cytoplasmic CTR aggregates (Figure 7B). No difference was observed between cervical and lumbar expression efficiency at any age or between ChAT-IRES-Cre;*Tardbp*$^{F/+}$ and ChAT-IRES-Cre;*Tardbp*$^{F/F}$ mice at p30, an early age preceding neuronal loss (Figure 7B), and CTR expression had no effect on Cre-mediated Tdp-43 knockout efficiency (Figure 1B). A small proportion of mice (~10%) that survived the initial injection later developed symptoms of hydrocephaly first appearing at p25-p30. The type of treatment (CTR versus GFP control injection) and genotype of the mouse did not affect risk of developing hydrocephaly, suggesting that this represented a delayed complication of the injection procedure itself and not a toxic side effect of CTR treatment. All mice displaying hydrocephaly symptoms were euthanized and excluded from analysis. While viral transduction was broadly distributed throughout the CNS, no behavioral or pathological evidence of acute or

chronic toxicity from transgenic protein expression was observed in any major organ system in GFP or CTR treated ChAT-IRES-Cre;*Tardbp*$^{F/+}$ mice at 12 months' age.

Treatment with CTR Attenuates Behavioral and Pathological Deficits in Mice lacking *Tardbp* in Motor Neurons

A cohort of ChAT-IRES-Cre;*Tardbp*$^{F/F}$ mice (Table 3) injected with our CTR fusion protein gained greater weight as compared to their untreated breeder-matched knockout controls (Figures 8B, 9). Treated ChAT-IRES-Cre;*Tardbp*$^{F/F}$ mice also performed better on the hanging wire and accelerating rotarod tests, with a delayed onset and slower progression of motor deficits (Figure 8C-E). Consequently, treated ChAT-IRES-Cre;*Tardbp*$^{F/F}$ mice showed a robust extending of their lifespan, with a median survival increase of 29 weeks, or 66 percent (Figure 8A). The increase in mortality in CTR-treated Tdp-43 knockout mice coincides in time with the loss of visible CTR accumulation (between 8 and 12 months), consistent with a therapeutic benefit of CTR. Notably, a cohort of ChAT-IRES-Cre;*Tardbp*$^{F/F}$ mice treated with just the N-terminal fragment of TDP-43 showed no such motor improvements, suggesting that splicing repression underlies the rescue effect (Figure 13).

Pathological analysis of a cohort of ChAT-IRES-Cre;*Tardbp*$^{F/+}$ and ChAT-IRES-Cre;*Tardbp*$^{F/F}$ mice revealed that while knockout mice lose 50% of ChAT-positive spinal motor neurons, CTR treatment significantly mitigated this motor neuron loss in both cervical and lumbar regions (Figure 10). Importantly, with our observed transduction efficiency of ~60%, this motor neuron rescue in CTR-treated ChAT-IRES-Cre;*Tardbp*$^{F/F}$ mice represents about 40% of the predicted

maximum cell-autonomous rescue effect (Figure 10B, dotted line). While L3 dorsal root area remained unchanged, L3 ventral spinal root cross-sectional area was also improved in treated ChAT-IRES-Cre;*Tardbp*$^{F/F}$ mice (Figures 10C, 11). No change in area of L3 dorsal or ventral roots in p30 mice of either genotype was observed. As predicted, treatment with our CTR protein re-repressed a subset of cryptic exon splicing events as determined by quantitative RT-PCR of cryptic exon targets previously identified*(Jeong et al., 2017)* (Figure 12). Taken together, our results support the idea that splicing repression is a major function of TDP-43 in motor neurons, suggest that loss of TDP-43-mediated splicing repression underlies neurodegeneration, and validate a novel mechanism-based therapeutic strategy for ALS.

Chapter 4: Discussion

Discussion

Although the association of TDP-43 pathology with ALS was disclosed a decade ago*(Arai et al., 2006b; Neumann et al., 2006)*, the major function of this RNA binding protein in motor neurons had remained undefined. We previously showed that TDP-43 helps maintain RNA fidelity by repressing aberrant splicing*(Ling et al., 2015)*. This function is compromised in the brains of cases of several neurodegenerative diseases, including ALS*(Ling et al., 2015; Sun et al., 2017b)*, suggesting that nuclear depletion of TDP-43 may underlie motor neuron degeneration. To target nuclear TDP-43 depletion as a potential therapeutic strategy to attenuate motor neuron disease, it is necessary to demonstrate that splicing repression is a major function of TDP-43 in motor neurons. This thesis project aimed to address this critical question. First, we confirmed that loss of neuronal Tdp-43 led to age-dependent neurodegeneration, behavioral deficits consistent with the phenotype of ALS/FTD, and compromised splicing repression in two different mouse models of TDP-43 loss of function. Next, to validate an AAV-based therapeutic strategy for ALS, we showed that the age-dependent motor neuron degeneration in Tdp-43 knockout mice could be mitigated by replenishing TDP-43 repression using an alternative splicing repressor protein, prolonging robustly the survival of mice lacking Tdp-43 in motor neurons. Our results were corroborated by complimentary work in Dr. Liam Chen's lab in which TBPH knockout flies transgenically expressing CTR showed similar improvements in survival, behavior, and splicing repression (unpublished). Hence, we establish for the first time *in vivo* that splicing repression is a major role of TDP-43 in motor neurons. Our results also validate a novel mechanism-based treatment strategy, in which virally-delivered spicing repressor comprised of the N-terminal fragment of TDP-43 (to recognize its RNA targets) fused to a well-

recognized splicing repressor (RAVER1) could potentially improve motor function and extend lifespan by restoring splicing repression in motor neurons of ALS patients. Given that nearly all cases of sporadic ALS display TDP-43 pathology*(Neumann et al., 2006)*, the lack of observable acute or chronic toxicity of the CTR repressor in mice would strongly support the therapeutic potential of our AAV-based treatment strategy in the clinic. To date, over 60 molecules representing at least 10 broadly defined mechanisms of action have been investigated as potential treatments for ALS*(Petrov, Mansfield, Moussy, & Hermine, 2017)*, but the overwhelming majority have failed to demonstrate efficacy in clinical trials. These failures over the last two decades are testament to the complexity of ALS and the lack of a unifying mechanism linking the various molecular and cellular observations in this disease. Our results help address this concern by validating a major function of an important disease-related protein, TDP-43, setting the stage for future gene therapy trials involving CTR or related variants.

The therapeutic relevance of our rescue approach is strengthened by the recent success of an AAV9-based Phase 1 gene therapy clinical trial for spinal muscular atrophy (SMA)*(Mendell et al., 2017)*. AAV vectors are currently the most common mode of transgene delivery for preclinical and clinical trials involving the CNS (for a review of different delivery methods, see Table 4) and are chosen primarily for their lack of cytotoxicity, broad host range, and episomal genetic incorporation*(McMenamin & Wood, 2010; Weinberg et al., 2013)*. While AAV is capable of transducing both dividing and non-dividing cells, transduction with AAV generally results in more robust expression in non-dividing cells such as neurons, as episomal genetic material is not replicated during mitosis*(Kaplitt et al., 1994)*. The AAV9 capsid serotype in particular

demonstrates neuronal tropism and is able to cross the blood-brain barrier when delivered systemically*(Chakrabarty et al., 2013; de Backer, Brans, Luijendijk, Garner, & Adan, 2010; Foust et al., 2009; Passini & Wolfe, 2001; Swain et al., 2014; Tanguy et al., 2015)*. Together, these characteristics of AAV9 make it a perfect candidate as a vehicle for future gene therapy studies to restore TDP-43 mediated splicing repression in humans.

Our neonatal AAV9-based delivery protocol allowed us to successfully transduce about 60 percent of ChAT-positive spinal motor neurons, a result consistent with other studies employing a similar delivery protocol and viral serotype*(McLean et al., 2014; H. Zhang et al., 2011)*. It is important to note that since our mouse model lacked Tdp-43 in >95% of ChAT-positive spinal motor neurons (Figure 1), we could not rescue all of these motor neurons, a limitation that likely hampered the magnitude of our rescue effect. Furthermore, that the splicing repressor domain of RAVER1 was not predicted to fully restore all TDP-43 dependent splicing events*(Ling et al., 2015)*, and that the observable accumulation of CTR protein was limited to 8-12 months are factors that likely undermined the outcome of this therapeutic strategy. Future experiments employing alternative splicing repressors, viral serotypes with higher neuronal tropism, such as AAV-PHP-eB*(Chan et al., 2017)*, and alternative delivery methods, such as intravenous or intrathecal injections in adult mice, will further validate the therapeutic benefit of our approach and help set the stage for future gene therapy clinical trials for ALS.

We previously demonstrated that cryptic exons are highly variable between different cell types and organisms, suggesting that TDP-43 loss may impair cell-type specific pathways in unique ways and complicating efforts at developing treatments targeting any particular final downstream pathway*(Jeong et al., 2017)*. However, the splicing repression function of TDP-43

is highly conserved across species*(Ling et al., 2015)*, making our mechanism-based therapeutic approach a more viable strategy. Furthermore, as mislocalization and nuclear clearance of TDP-43 occurs in a subset of patients with frontotemporal dementia*(Neumann et al., 2006)*, inclusion body myopathy*(Salajegheh et al., 2009)*, and Alzheimer's disease*(Amador-Ortiz et al., 2007)*, our mechanism-based strategy may hold promise for these diseases as well.

Our results do not exclude other putative function of TDP-43, as this protein has been implicated in a variety of important nuclear and non-nuclear cellular processes besides splicing repression, nor do they address the potential toxic effects of cytoplasmic TDP-43 aggregation on disease progression. Nuclear TDP-43 depletion is an early event, possibly preceding its cytoplasmic aggregation*(Vatsavayai et al., 2016b)*, and while promising therapeutic options for reducing TDP-43 aggregation mediated toxicity are being developed*(Becker et al., 2017a)*, further effort is needed to clarify the different contributions of toxic gain of function and nuclear loss of function of TDP-43 to the pathogenesis of neurodegenerative diseases. Assessing the importance of splicing repression in other models of neuronal TDP-43 dysfunction, such as one expressing transgenic TDP-43 with a nonfunctional nuclear localization sequence that sequesters endogenous Tdp-43*(Spiller et al., 2016)* will improve our understanding of the complex interplay between cytoplasmic accumulation and nuclear loss of TDP-43.

In summary, we show that restoring splicing repression in TDP-43 deficient motor neurons in mice prolongs survival and attenuates motor neuron disease. Our study not only establishes a major role of TDP-43 in motor neurons but also validates a novel mechanism-based therapeutic target for ALS and other diseases exhibiting TDP-43 pathology.

Figures and Tables

Table 1: List of motor neuron diseases

Name	Description	Upper Motor Neurons Affected?	Lower Motor Neurons Affected?
Amyotrophic Lateral Sclerosis (ALS)	Unknown cause in 90-95 percent of cases (termed sALS). Characterized by death of upper and lower motor neurons, muscle weakness, spasticity, and loss of voluntary control*(Cleveland et al., 2001; del Aguila et al., 2003; Julien, 2001)*	Yes	Yes
Primary Lateral Sclerosis (PLS)	Diagnosis of exclusion; unclear if actually a slowly progressing form of ALS*(Pringle et al., 1992; Wais et al., 2017)*	Yes	No
Hereditary Spastic Paraplegia (HSP)	Progressive spasticity in lower limbs that can be inherited in autosomal dominant (~43%), recessive (~10%), or simplex (~47%)*(Sch**le et al., 2016)*	Yes	No
Spinal Muscular Atrophies (SMAs, most commonly autosomal recessive SMA)	90-95% of cases involve genetic mutations of *SMN1* gene, inducing death of lower motor neurons and muscle atrophy*(Lim & Hertel, 2001; Lorson, Hahnen, Androphy, & Wirth, 1999)*	No	Yes
Progressive Bulbar Palsy	Affects neurons innervating bulbar muscles*(Swash & Desai, 2000)*	No	Yes
Pseudobulbar Palsy	Spasticity of bulbar muscles caused by damage to corticobulbar tract*(Grattan-Smith, Hopkins, Shield, & Boldt, 1989)*	Yes	No

Table 2: Genetics of ALS(Boylan, 2015; Cirulli et al., 2015a; Taylor, Brown, & Cleveland, 2016)

Gene	Protein	Chromosome Locus	Phenotype	Displays TDP-43 pathology
ALS2*(Polymenidou et al., 2011; Y. Yang et al., 2001)*	Alsin	2q33.1	Juvenile ALS	Yes
ANG*(Paubel et al., 2008)*	Angiogenin	14q11.2	ALS, Parkinson's Disease	Unknown
ANXA11(Smith et al., 2017)	Annexin A11	10q22.3	ALS	Yes
ATXN2*(Becker et al., 2017a; Elden et al., 2010)*	Ataxin-2	12q24.12	ALS, Spinocerebellar ataxia 2, parkinsonism	Yes
C21ORF2*(van Rheenen et al., 2016)*	Leucine-rich repeat containing protein 76	21q22.3	ALS, retinal dystrophy	Unknown
C9ORF72*(Chew et al., 2015; Renton et al., 2011)*	C9ORF72	9p21	ALS, ALS-FTD, FTD	Yes
CCNF(Williams et al., 2016)	Cyclin F	16p33.3	ALS, ALS-FTD, FTD	Yes
CHMP2B*(Cox et al., 2010; Parkinson et al., 2006)*	Chromatin-modifying protein 2b	3p11.2	ALS, ALS-FTD, FTD	Yes
DCTN1*(Konno et al., 2017)*	Dynactin	2p13	FTD, Perry Syndrome	Yes (Perry Syndrome)
FIG4*(Chow et al., 2009; Kon et al., 2014)*	Polyphosphoinositide phosphatase	6q21	ALS	Yes
FUS*(Baumer et al., 2010; Urwin et al., 2010; Vance et al., 2009)*	Fused in sarcoma	16p11.2	ALS, Juvenile ALS, FTD	No

MATR3*(Johnson et al., 2014)*	Matrin-3	5q31.2	ALS, distal myopathy 2	Yes
MOBP(van Rheenen et al., 2016)	Myelin associated oligodendrocyte basic protein	3p22.1	ALS, progressive supranuclear palsy	Unknown
NEFH*(Al-Chalabi et al., 1999)*	Neurofilament heavy	22q12.2	ALS, sensory neuropathy	Unknown
NEK1*(Kenna et al., 2016)*	NIMA-related kinase	4q33	ALS, retinal dystrophy	Yes
OPTN*(Yamashita et al., 2013)*	Optineurin	10p13	ALS, glaucoma	Yes
PFN1*(Tanaka & Hasegawa, 2016; C. Wu et al., 2012)*	Profilin-1	12p13.2	ALS	Yes
PRPH*(Corrado et al., 2011)*	Peripherin	12q13.12	ALS	Unknown
SCFD1(van Rheenen et al., 2016)	Syntaxin-binding protein 1	14q12	ALS	Unknown
SETX*(Hirano et al., 2011)*	Senataxin	9q34	SCA 1, ALS	No, but implicated in RNA processing
SOD1*(Jones et al., 1993; Mackenzie et al., 2007)*	Cu/Zn superoxide dismutase-1	21q22.1	ALS, progressive muscular atrophy	No
SQSTM1*(Brady, Meng, Zheng, Mao, & Hu, 2011; Fecto et al., 2011)*	p62/sequestome	5q35.3	ALS, FTD	Yes
TARDBP*(Arai et al., 2006b; Neumann et al., 2006; Rutherford et al., 2008)*	Tar DNA-binding protein 43 (TDP-43)	1p36.2	ALS, ALS-FTD, FTD, Inclusion body myopathy	Yes

TBK1*(Cirulli et al., 2015b; Freischmidt et al., 2015)*	TANK-binding kinase 1	12q14.2	ALS	Yes
TREM2*(Cady et al., 2014)*	TREM-2	6p21.1	ALS, AD, Parkinson's disease. Nasu-Hakola disease	Yes (AD)
TUBA4A*(Smith et al., 2014)*	Tubulin alpha 4a	2q35	ALS, ALS-FTD, FTD	Yes
UBQLN2*(Hanson, Kim, Wassarman, & Tibbetts, 2010)*	Ubiquilin2	Xp11	ALS, FTD	Yes
VAPB*(Kanekura, Nishimoto, Aiso, & Matsuoka, 2006)*	VAMP-associated protein B	20q13.32	ALS, progressive muscular atrophy	Yes
VCP*(Johnson et al., 2010; Neumann et al., 2007)*	VCP	9p13.3	ALS, ALS-FTD, FTD, Inclusion body myopathy	Yes
VEGFA*(Lambrechts et al., 2003; Shantanu et al., 2017)*	Vascular endothelial growth factor	6p21.1	ALS	Yes

Table 3: Sample size for CTR rescue experiment(s)

	ChAT-IRES-Cre;Tardbp$^{F/F}$ **CTR Injected**	ChAT-IRES-Cre;Tardbp$^{F/F}$ **GFP Injected**	ChAT-IRES-Cre;Tardbp$^{F/+}$ **CTR Injected**	ChAT-IRES-Cre;Tardbp$^{F/+}$ **GFP Injected**
Cohort 1	11 (2♀)	11 (7♀)	8 (3♀)	8 (5♀)
Cohort 2	9 (6♀)	11 (3♀)	12 (6♀)	6 (2♀)
P90 pathology analysis cohort	6 (3♀)	6 (3♀)	5 (3♀)	4 (3♀)

	ChAT-IRES-Cre;Tardbp$^{F/F}$ **NT Injected**	ChAT-IRES-Cre;Tardbp$^{F/F}$ **GFP Injected**	ChAT-IRES-Cre;Tardbp$^{F/+}$ **NT Injected**	ChAT-IRES-Cre;Tardbp$^{F/+}$ **GFP Injected**
N-terminal fragment cohort	6 (2♀)	3(2♀)	4 (2♀)	4 (2♀)

Table 3: Final sample sizes for all mouse cohorts examined in this study, separated by genotype and injection type.

Table 4: Gene therapy delivery vehicles for preclinical and clinical CNS disease therapeutic trials (Donde, Wong, & Chen, 2017)

Delivery Vehicle	Benefits	Drawbacks
Adeno-associated virus (AAV)*(Burger et al., 2004; Chakrabarty et al., 2013; de Backer et al., 2010; Foust et al., 2009; Howard et al., 2008; Kaplitt et al., 1994)*	Wide variety of pseudotypes for neuron and glia-specific targeting Robust expression after several months Episomal incorporation reduces risk of harmful insertion Some serotypes can cross BBB when injected systemically	~4.5 kb carrying capacity complicates large/multiple transgenes and CRISPR delivery Reactive astrogliosis possible Expensive to produce Episomal incorporation is less efficient in dividing cells Safety concerns about mutations restoring viral replication competency
Retrovirus*(Cannon, Sew, Montero, Burton, & Greenamyre, 2011; Cockrell & Kafri, 2007; Evans & Garcia, 2000; Naldini, Blmer, Gage, Trono, & Verma, 1996)*	Larger carrying capacity (~9 kb) Easier and cheaper to produce than AAV Wide variety of pseudotypes for neuron and glia-specific targeting Insertion into host genome allows transduction of replicating cells	Safety concerns about insertional mutagenesis Safety concerns about mutations restoring viral replication competency Does not cross BBB when injected systemically Reactive astrogliosis possible
In-utero electroporation*(Davtyan et al., 2012; Taniguchi, Young-Pearse, Sawa, & Kamiya, 2012)*	Cheaper to produce than viral vectors Limited cell type targeting based on timing of electroporation Low immuogenicity	Limited to prenatal animal models Episomal incorporation is less efficient in dividing cells
Synthetic vectors*(Aktas et al., 2005; Koltover, Salditt, Rdler, & Safinya, 1998; Mamot et al., 2004; Pack, Hoffman, Pun, & Stayton, 2005; Shyam et al., 2015)*	Cheaper to produce than viral vectors Low immunogenicity >10kb carrying capacity	More transient expression profile Low *in-vivo* efficiency
Antisense oligonucleotides*(Aartsma-*	Cheap and easy to produce	Can only modify endogenous transcripts

Rus, 2017; Becker et al., 2017b; Corey, 2017; DeVos et al., 2013; Donnelly et al., 2013; Miller et al., 2013; Passini et al., 2011)	Widespread cellular uptake in the CNS	Cannot easily cross the BBB when delivered systemically Potential off-target toxicity

Figure 1: Deletion of Tdp-43 in lower motor neurons of mice

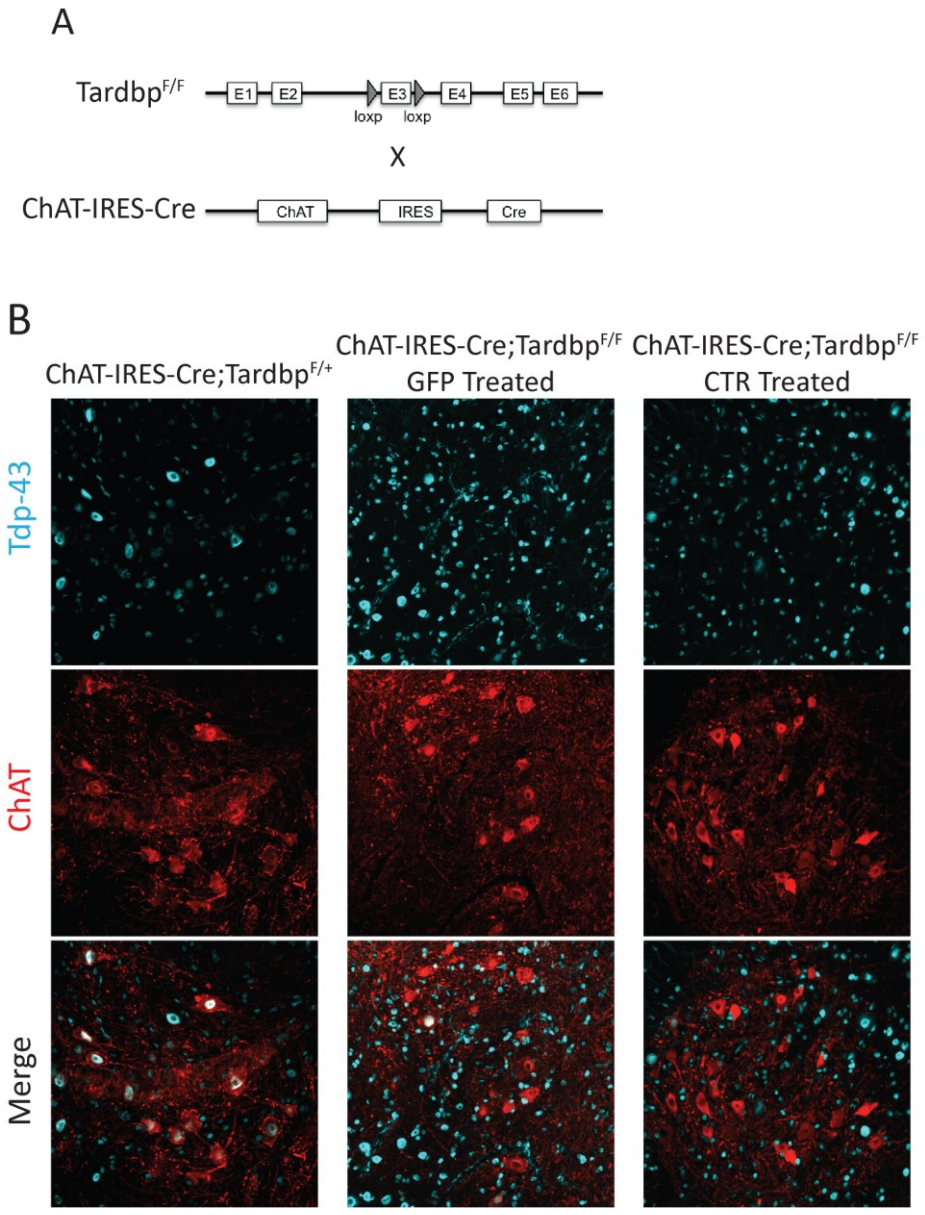

Figure 1 Legend: **(A)** Schematic of ChAT-IRES-Cre and Tardbp$^{F/F}$ alleles in our conditional Tdp-43 knockout mouse. Cre-mediated excision of exon 3 leads to nonsense-mediated decay of the mRNA transcript. **(B)** Immunofluorescent stain of ChAT (red) and Tdp-43 (blue) in p30 ChAT-IRES-Cre;Tardbp$^{F/+}$ mice, CTR treated and untreated ChAT-IRES-Cre;Tardbp$^{F/F}$ mice. In all three groups, Cre-dependent Tdp-43 knockout rate was ~95% in both cervical and lumbar sections and not significantly different between groups.

Figure 2: Loss of Tdp-43 in lower motor neurons leads to age-dependent neurodegeneration

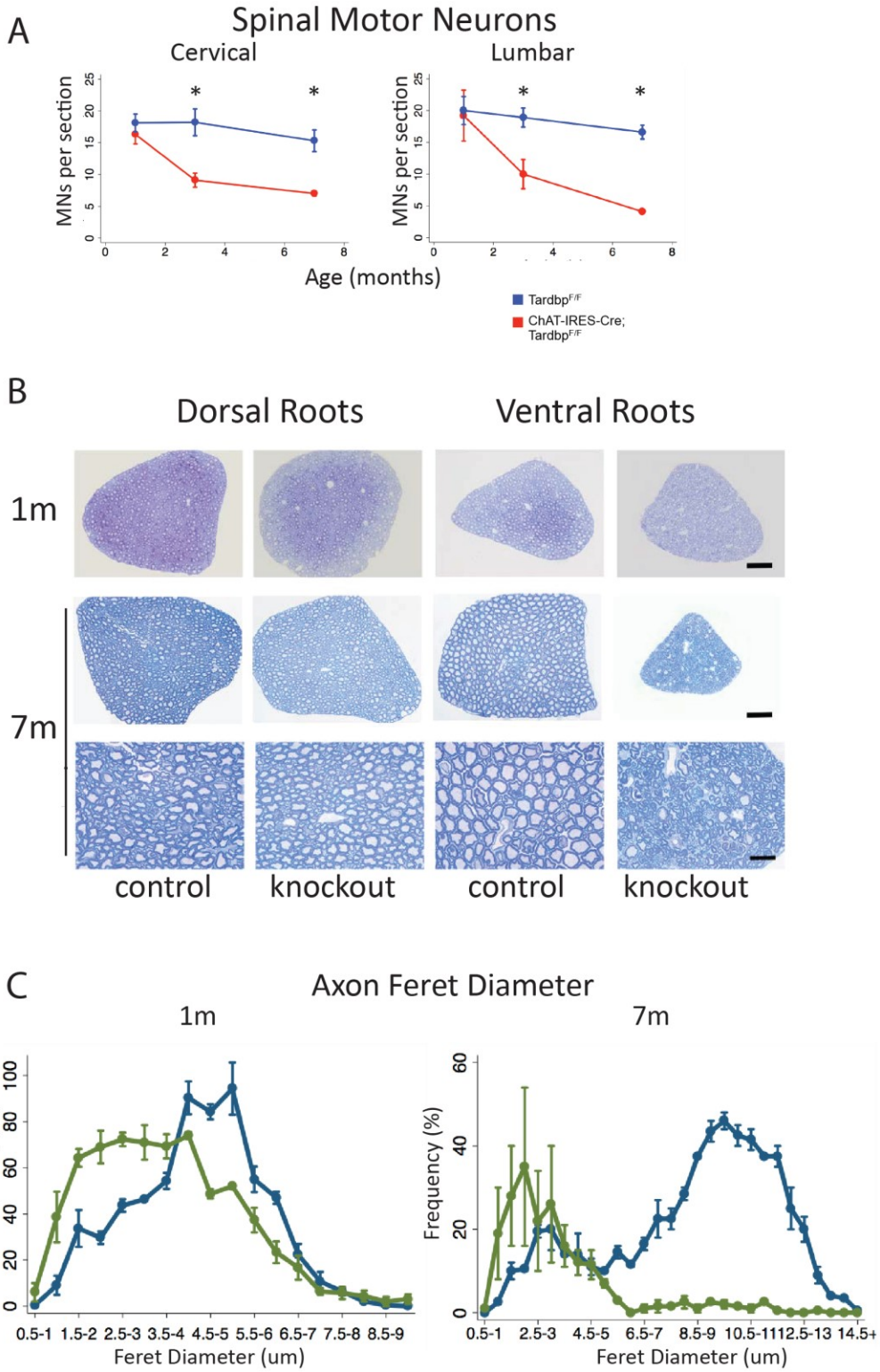

Figure 2 Legend: **(A)** Progressive motor neuron loss in *ChAT*-IRES-Cre;*Tardbp*$^{F/F}$ mice; lumbar spinal sections were immunostained against ChAT (see Figures 9 and 10 for examples). Few ChAT-positive neurons remain in the ventral horn of 7-month-old knockout mice (*$p < 0.05$). **(B)** Transverse sections of L4 dorsal and ventral roots. Loss of large motor axons in the ventral roots of 7 month old *ChAT*-IRES-Cre;Tardbp$^{F/F}$ mice is evident. No change is observed at 1 month Scale bar: 50μm, first and second panels, 20μm, third panel. **(C)** Distribution of ventral root axon feret diameter at 1 and 7 months for *ChAT*-IRES-Cre;Tardbp$^{F/F}$ mice (green) and *ChAT*-IRES-Cre;Tardbp$^{F/+}$ control mice (blue). The total number of axons was unchanged at 1 month and significantly reduced (574±40 vs 425±23 axons, $p < 0.05$, $n = 5$)*(LaClair et al., 2016)*.

Figure 3: Inducible deletion of Tdp-43 in excitatory forebrain neurons in mice

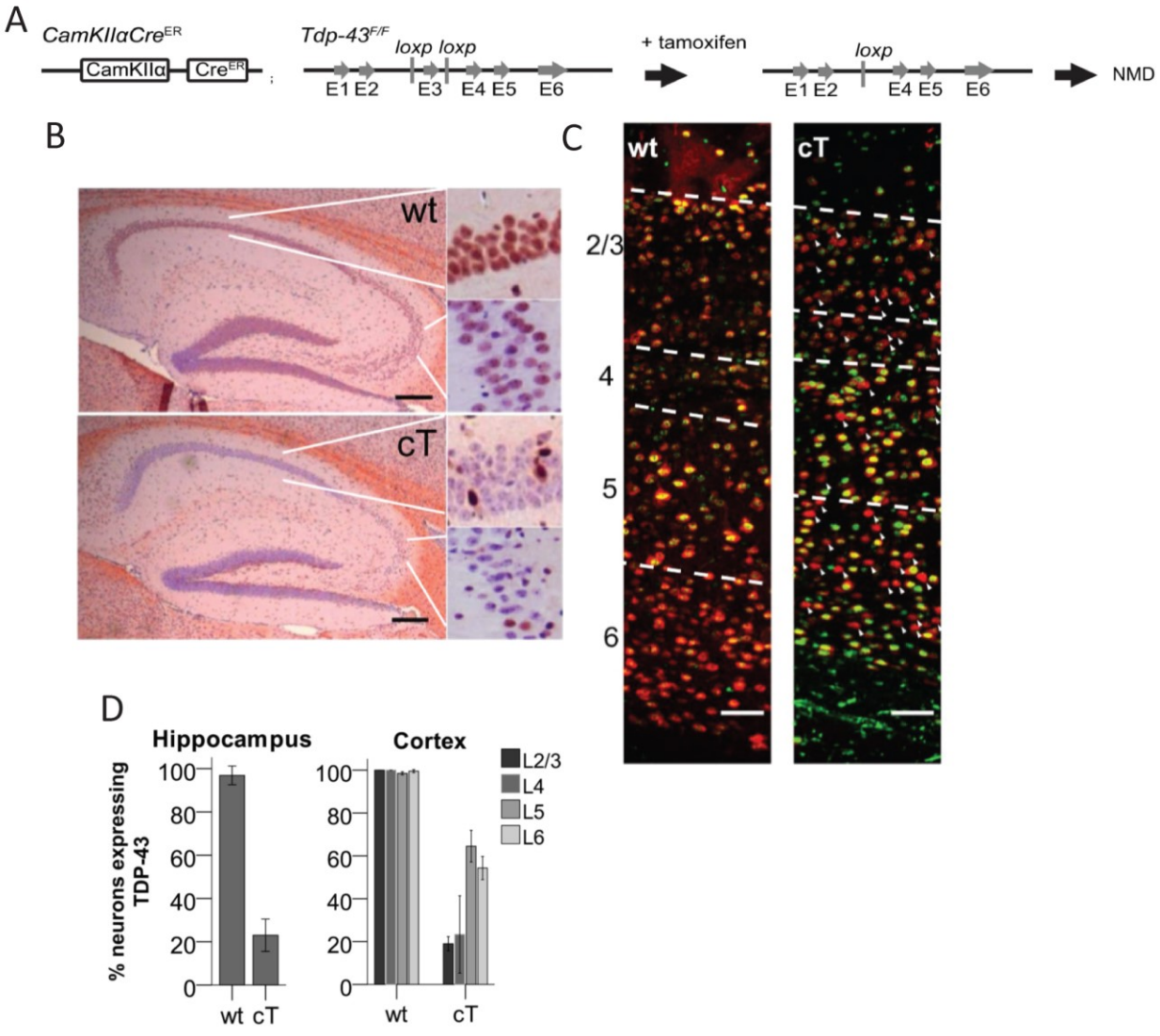

Figure 3 Legend: **(A)** Gene diagram of CaMKIIa-Cre^{ER} and Tdp-43$^{F/F}$ alleles. Administration of tamoxifen leads to Cre-mediated excision of Tdp-43 exon 3, and subsequent mRNA degradation through nonsense mediated decay (NMD). **(B)** TDP-43 N-terminal (red) with hematoxylin counterstain (blue) for representative CaMKIIa-Cre^{ER};Tardbp$^{F/+}$ control mice (termed 'wt') and CaMKIIa-Cre^{ER};Tardbp$^{F/F}$ knockout mice (termed 'cT') sections at 3 months of age in the hippocampus. **(C)** TDP-43 C-terminal (green) and NeuN (red) staining in the frontal cortex of representative sections from wt and cT mice. Dashed lines mark the boundaries of the cortical layers, numbered on the left side. Arrowheads indicate some neurons (NeuN, red) without visible TDP-43 staining. Scale bars b 200 µm, c 100 µm. **(D)** Quantifications of % neurons (NeuN+) expressing detectable TDP-43 in the hippocampus and the cortical layers of wt and cT at 3 months of age. TDP-43 is lost in 80% of pyramidal neurons in the hippocampus and cortex layers 2/3 and 4, and ~40% of pyramidal neurons in cortex layers 5 and 6 (N = 6 wt, 5 cT)*(LaClair et al., 2016)*.

Figure 4: Neuronal loss in inducible forebrain Tdp-43 knockout mice

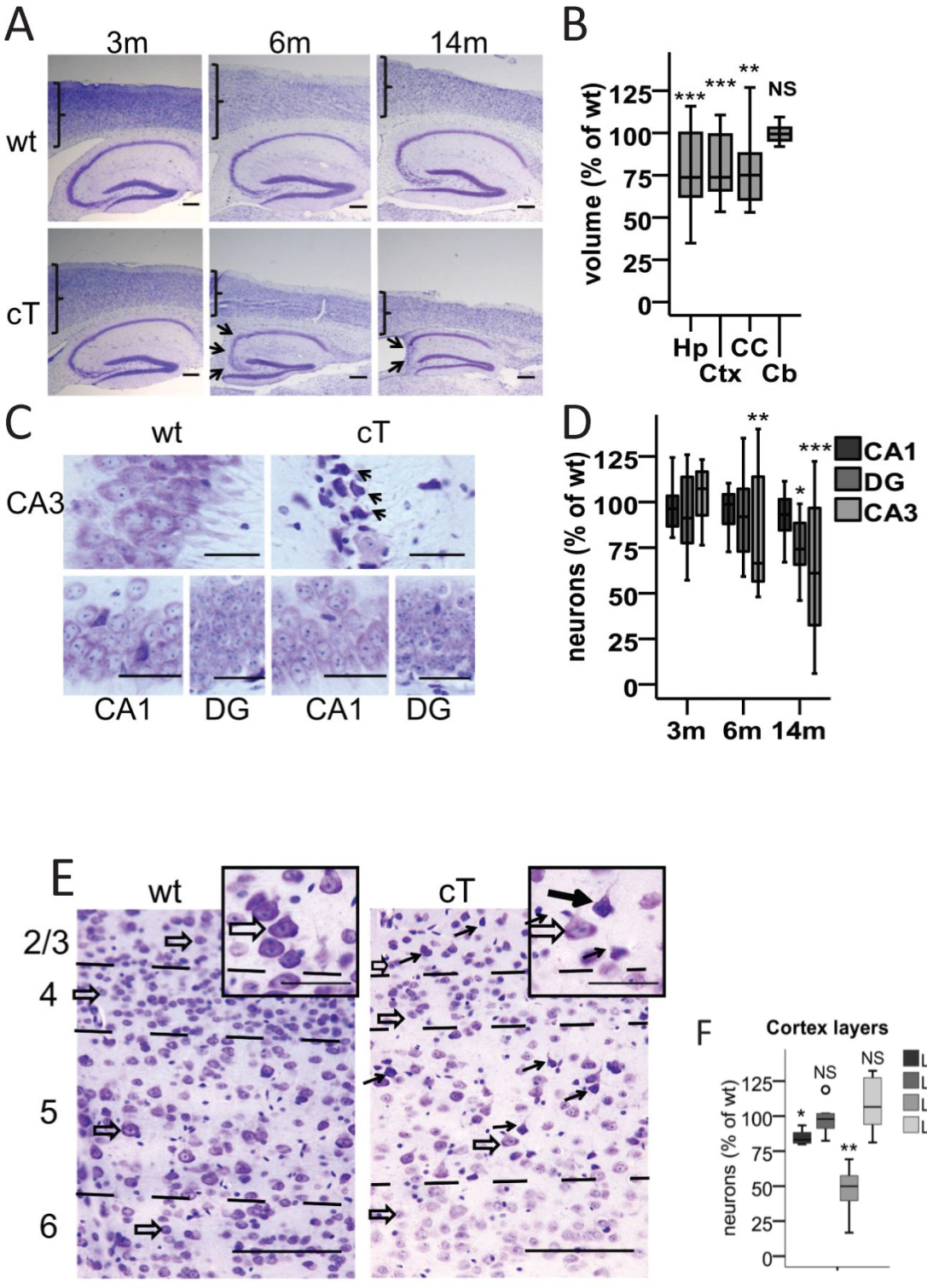

Figure 4 Legend: Tdp-43 loss leads to selective vulnerability in hippocampal CA3/2 and cortical Layer II/III and V neurons, and cognitive and behavioral abnormalities. **(A)** Progressive hippocampal and cortical atrophy in cT mice, with cortical thinning and severe CA3/2 cell loss (arrows) at indicated ages. **(B)** Regional volume in cT mice is reduced in hippocampus (Hp) [$F(1,11) = 18.836$, *** $p = 0.001$], cortex (Ctx) [$F(1,11) = 46.435$, *** $p < 0.001$], and corpus callosum (CC) [Welch(1,5.505) = 19.470, ** $p = 0.001$], but not cerebellum (Cb) [$F(1,11) = 0.066$, $p = 0.803$], compared to wt at 8 months (n : wt = 5, ct = 8). **(C)** Selective degeneration of CA3/2 neurons in cT mice (some indicated by arrows) at 4 months, while CA1 and DG are unaffected. **(D)** CA3/2 neurons are selectively lost at 6 months [$t(10) = 3.428$, ** $p = 0.002$; wt ($M = 182.42$, $SD = 54.41$), cT ($M = 104.62$, $SD = 11.37$)], followed by the dentate gyrus (DG) at 14 months ($t(14) = 2.339$, * $p = 0.035$) while CA1 neurons are unchanged [$t(14) = 1.843$, $p = 0.087$]. (3 and 6 m n = 6; 14 m n = 8). **(E)** CV staining in the cortical layers at 3 months of age. Degenerating neurons (black arrows) are numerous in layers III and V of cT mice, in contrast to normal neurons (open arrows). Insets show magnified healthy (open arrows) vs degenerating neurons (black arrows) in layer V. **(F)** Quantification of morphologically healthy neurons revealed that neurons degenerate significantly in cortical layers 2/3 and 5, but not 4 and 6 in 3-month-old cT mice compared to wt. [Layer 2/3 $F(1,7) = 11.653$, $p = 0.011$*; Layer 4 $F(1,7) = 0.046$, $p = 0.836$ NS; Layer 5 $F(1,7) = 23.399$, $p = 0.002$**; Layer 6 $F(1,7) = 0.354$, $p = 0.570$ NS] (wt = 3, cT = 6). Outliers = ○ *(LaClair et al., 2016)*.

Figure 5: Behavioral deficits in inducible forebrain Tdp-43 knockout mice

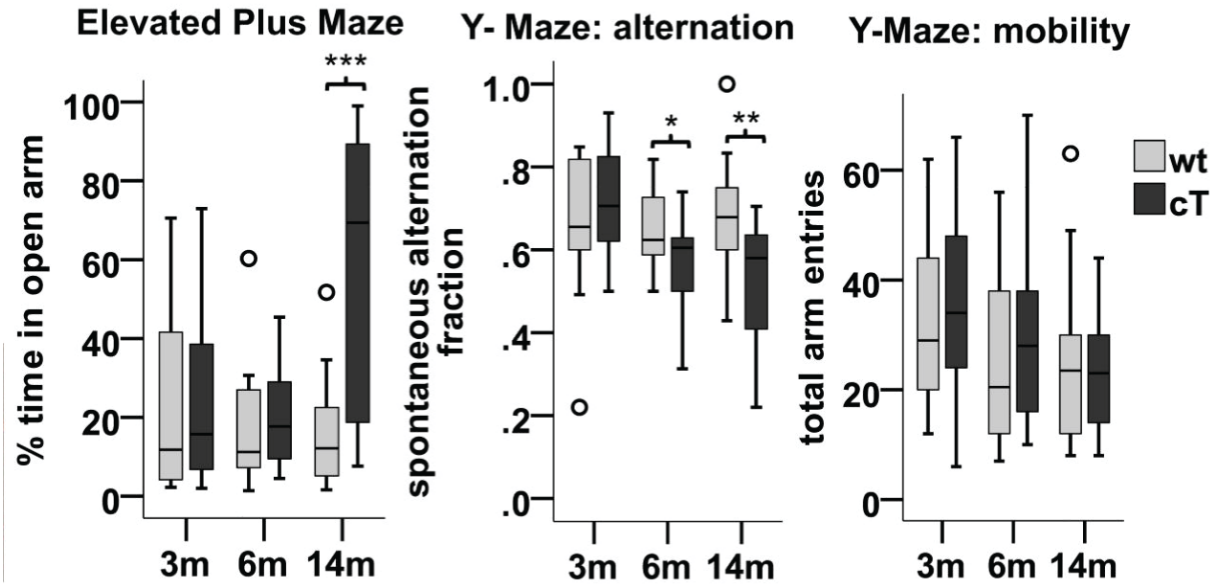

Figure 5 Legend: Performance of cT and wt mice in the elevated plus maze and the Y-maze. Left cT mice show increased time in the open arm of the elevated plus maze by 14 months of age compared to wt littermates ($p < 0.001$). Middle cT mice show significantly reduced spontaneous alternation in the Y-maze by 6 months of age compared to wt littermates ($p = 0.043$). Right total number of arm entries in the Y-maze does not differ between cT and wt mice, even at 14 m ($p = 0.821$) (Outliers = ○) (3m and 6m n = 14/group; 14m n = 17/group) *(LaClair et al., 2016)*.

Figure 6: Cryptic exon incorporation in inducible forebrain neuron Tdp-43 knockout mice

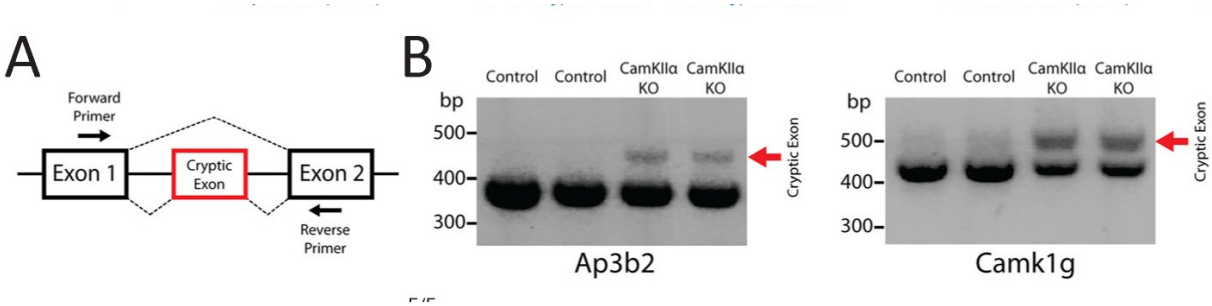

Figure 6 legend: **(A)** Schematic showing the locating of the cryptic exon and primers in adjacent annotated exons (not to scale). **(B)** RT-PCR validation of two cryptic exons (red arrows) in the Ap3b2 and Camk1g transcripts in RNA extracted from hippocampi of 3 month old CaMKIIα-Cre;Tardbp$^{F/F}$ mice.

Figure 7: Robust CTR expression in motor neurons of mice

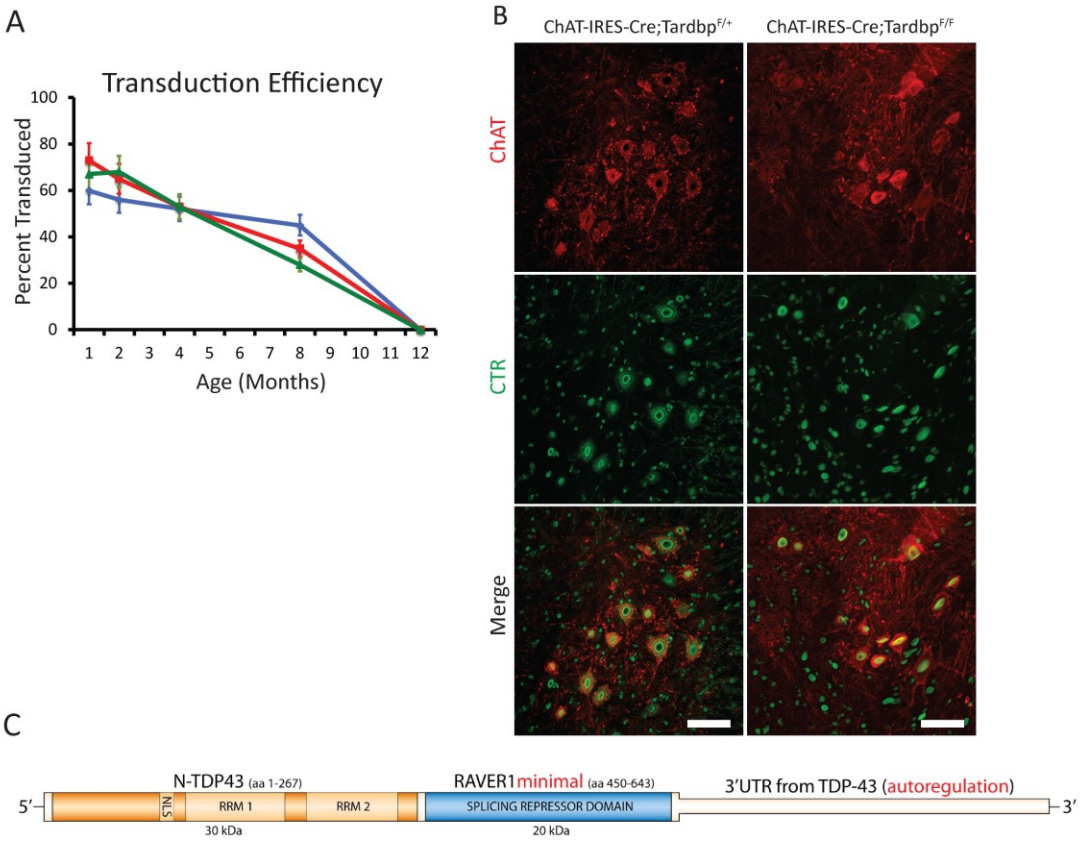

Figure 7 Legend: **(A)** Quantification of nuclear CTR in ChAT-positive neurons in ChAT-IRES-Cre;Tardbp$^{F/+}$ mice in cervical (green), lumbar (red), and dorsal horn neurons (blue). Our protocol allowed for a ~60% efficiency of targeting motor neurons until at least 8 months, with no difference observed between cervical and lumbar regions. (N=3 animals per time point, 5 spinal sections per region per animal, scale bar = 100 μm). **(B)** Immunostaining of ChAT (red) and CTR (recognized by human-specific N-terminal TDP-43 antibody, green) in representative lumbar ventral horn sections of ChAT-IRES-Cre;Tardbp$^{F/+}$ and ChAT-IRES-Cre;Tardbp$^{F/F}$ mice. **(C)** Diagram of the CTR chimeric protein construct packaged in AAV9, with the N-terminal fragment of human TDP-43 (orange), the splicing repression domain of RAVER1 (blue), and the 3' untranslated region (3'UTR) from human TDP-43.

Figure 8: CTR expression delays onset and progression of symptoms and prolongs survival

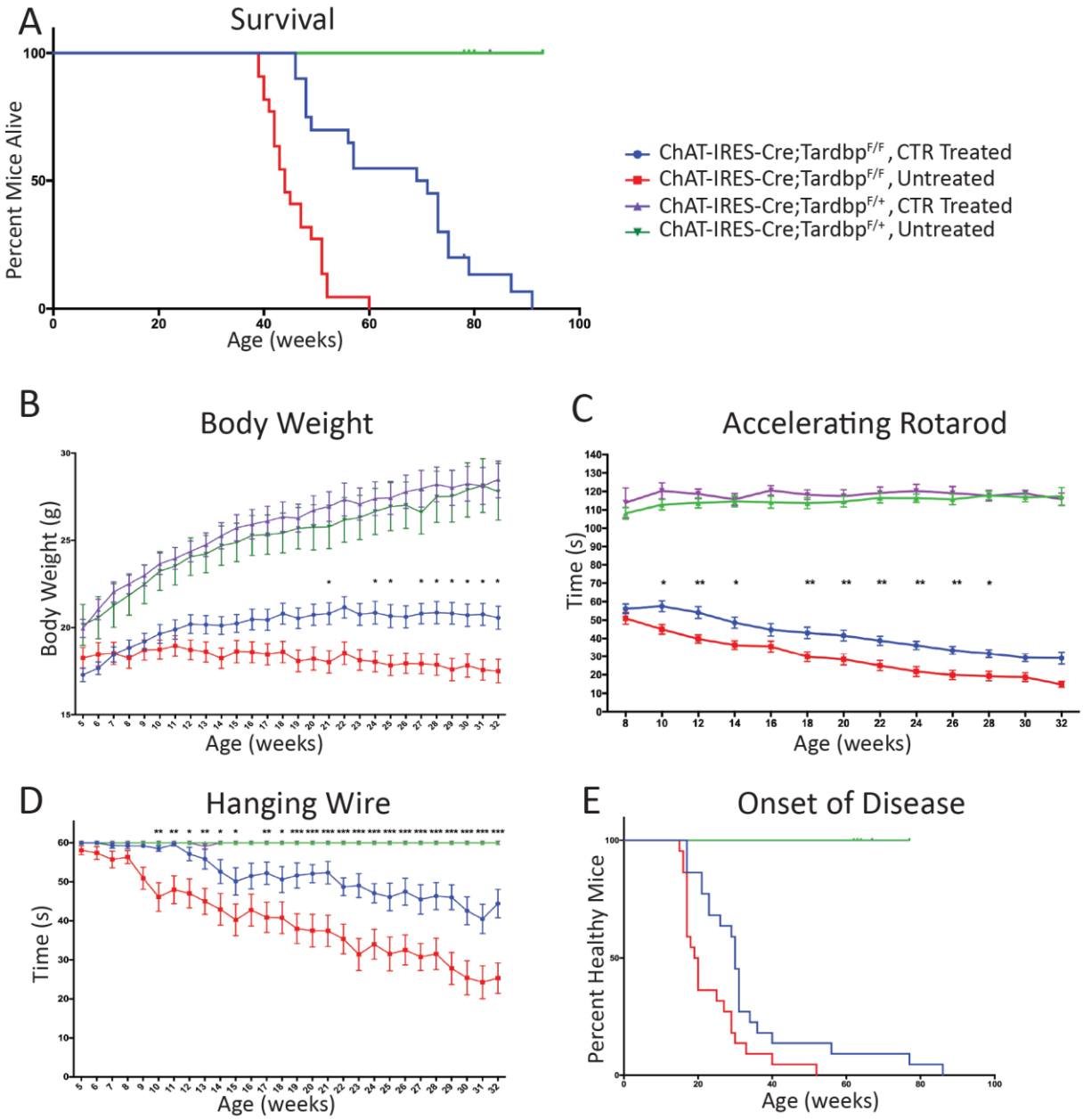

Figure 8 Legend: Expression of CTR in Tdp-43 knockout mice prolong survival and attenuates behavioral deficits. **(A)** Kaplan-Meier survival curve of ChAT-IRES-Cre;Tardbp$^{F/+}$ and ChAT-IRES-Cre;Tardbp$^{F/F}$ mice administered AAV9 containing either CTR (treated) or GFP control (untreated). Data from both cohorts are shown together. Median untreated ChAT-IRES-Cre;Tardbp$^{F/F}$ survival was extended from 44 weeks to 73 weeks in treated mice ($p < 0.001$ for all analyses). **(B)** CTR treatment mitigated the age-dependent body weight loss of knockout mice while having no effect on control mice. Hanging wire **(C)** and rotarod performance **(D)** show a mitigation of motor deficits in CTR-treated knockout mice compared to untreated controls (*$p < 0.05$, ** $p < 0.01$, *** $p < 0.001$, Tukey's multiple comparison test). Progression of hanging wire deficits was also significantly attenuated in CTR-treated mice (untreated slope=-1.19, CTR slope= -0.68, $p < 0.01$) **(E)** Kaplan-Meier survival curve of onset of motor dysfunction, as defined as two consecutive weeks of <60s hanging wire time. Onset was delayed in CTR-treated knockout mice (median onset: 30 versus 19 weeks, $p < 0.001$).

Figure 9: Differences in bodyweight for males and females

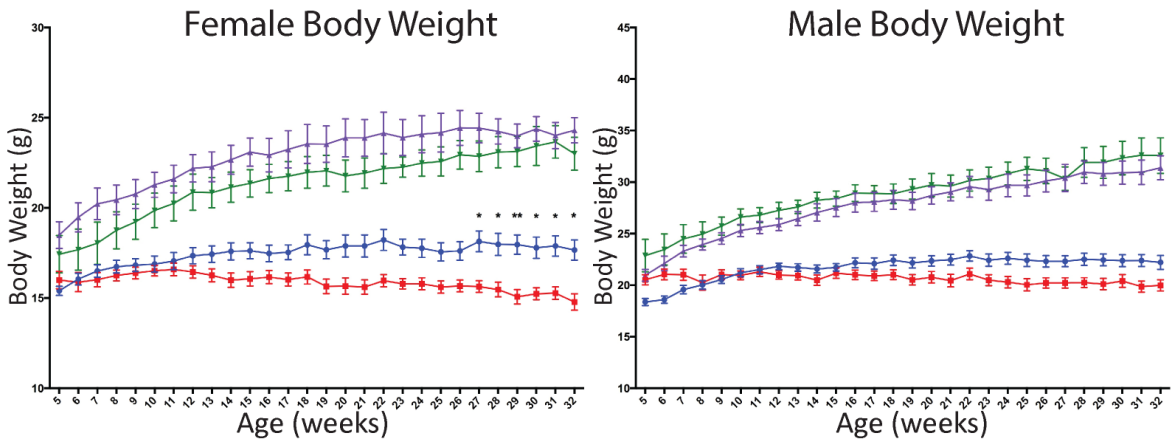

Figure 9 Legend: Body weights for CTR treated and untreated ChAT-IRES-Cre;Tardbp$^{F/+}$ and ChAT-IRES-Cre;Tardbp$^{F/F}$ mice, separated by sex (* $p < 0.05$, ** $p < 0.01$).

Figure 10: Attenuation of pathological deficits in p90 CTR-treated knockout mice

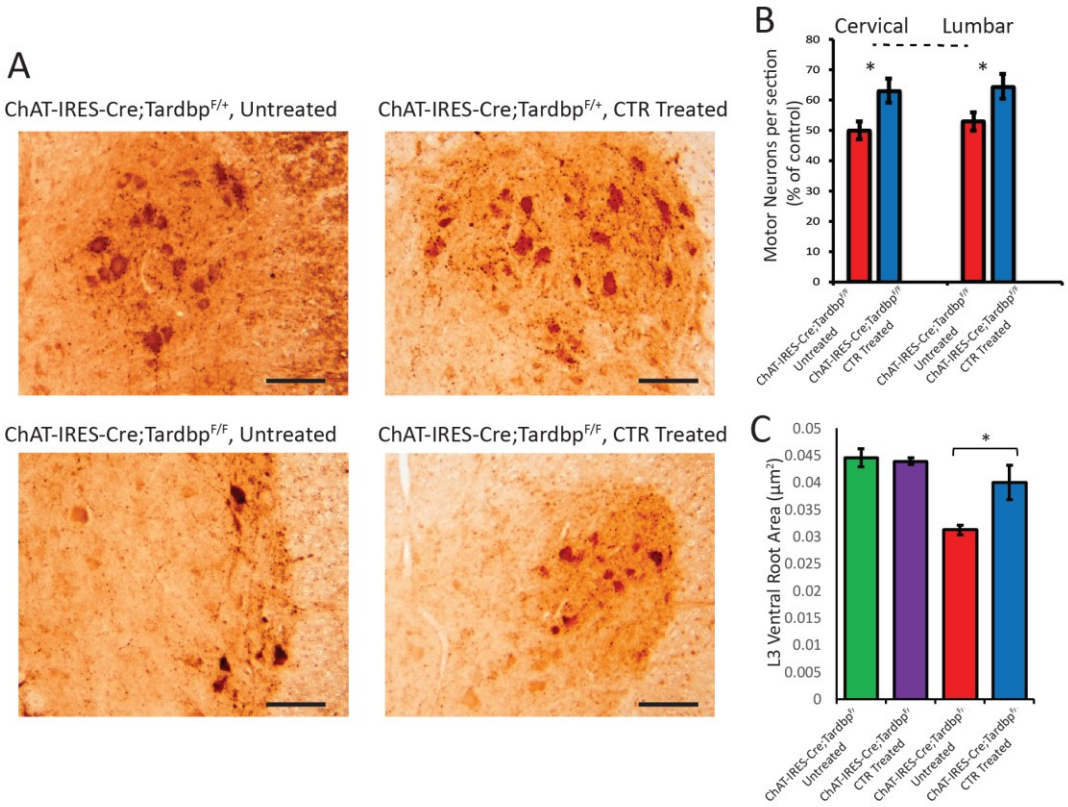

Figure 10 Legend: Expression of CTR in Tdp-43 knockout mice attenuates motor neuron loss and restores splicing repression. **(A)** Representative ChAT immunostaining of an L3 lumbar ventral horn section. (scale bar = 100 µm). **(B)** Quantification of ChAT-positive motor neurons in CTR-treated (blue) and untreated (red) knockout mice. As no difference was observed between CTR-treated and untreated ChAT-IRES-Cre;Tardbp$^{F/+}$ mice, results are shown as a percentage of each group's respective control. Untreated knockout mice showed a 50% decrease in motor neuron number at p90, whereas the motor neuron abundance of CTR-treated knockout mice is 63% (lumbar) and 61% (cervical) of controls (*$p < 0.05$). With a transduction efficiency of 60 percent, a complete cell-autonomous rescue of motor neuron death by CTR would still only result in a motor neuron rescue of ~80% (dashed line). **(C)** Quantification of cross-sectional area. Ventral, but not dorsal, root area was diminished in untreated ChAT-IRES-Cre;Tardbp$^{F/F}$ mice and restored with CTR treatment (* $p < 0.05$).

Figure 11: Representative dorsal and ventral roots of p90 mice

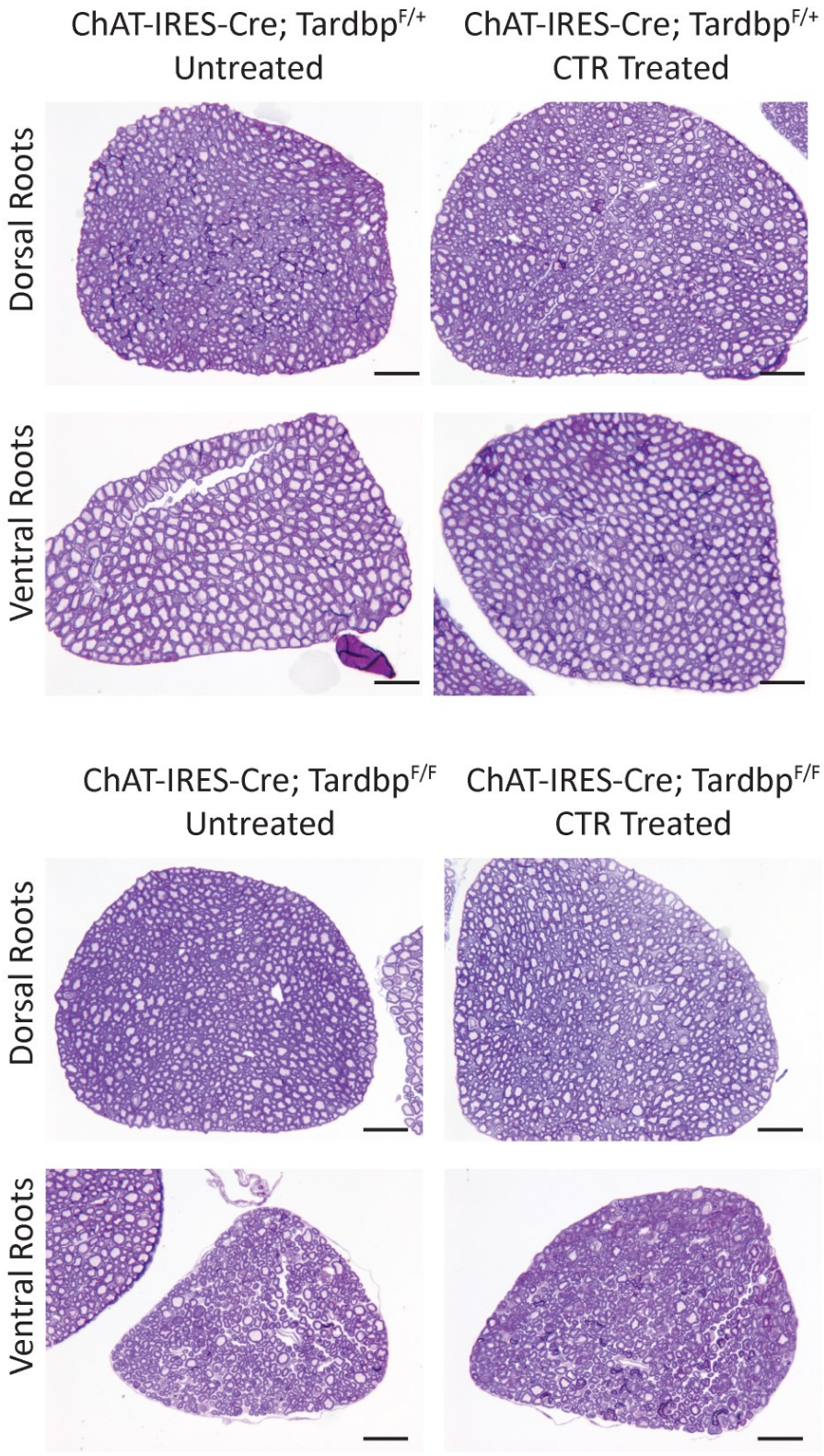

Figure 11 Legend: Representative cresyl violet stained dorsal and ventral L3 roots. Ventral, but not dorsal, root area was diminished in untreated ChAT-IRES-Cre;Tardbp$^{F/F}$ mice and restored with CTR treatment (scale bar = 200 μm)

Figure 12: Restoration of normal splicing repression

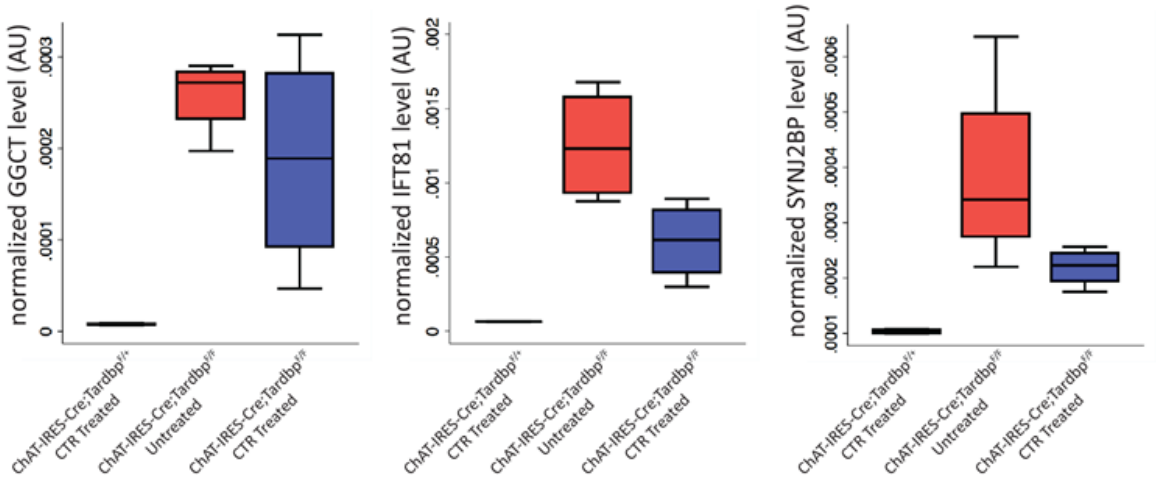

Figure 12 Legend: Relative levels of three cryptic exon mRNA targets predicted to be incorporated in Tdp-43 deficient motor neurons in p45 mice, normalized to an average of GAPDH and TBP genes as determined by quantitative RT-PCR. A reduction in SYNJ2BP and IFT81 cryptic exon incorporation (but not GGCT) was observed in CTR-treated ChAT-IRES-Cre;Tardbp$^{F/F}$ mice (* $p < 0.05$, one-way ANOVA).

Figure 13: N-terminal fragment alone has no therapeutic benefit

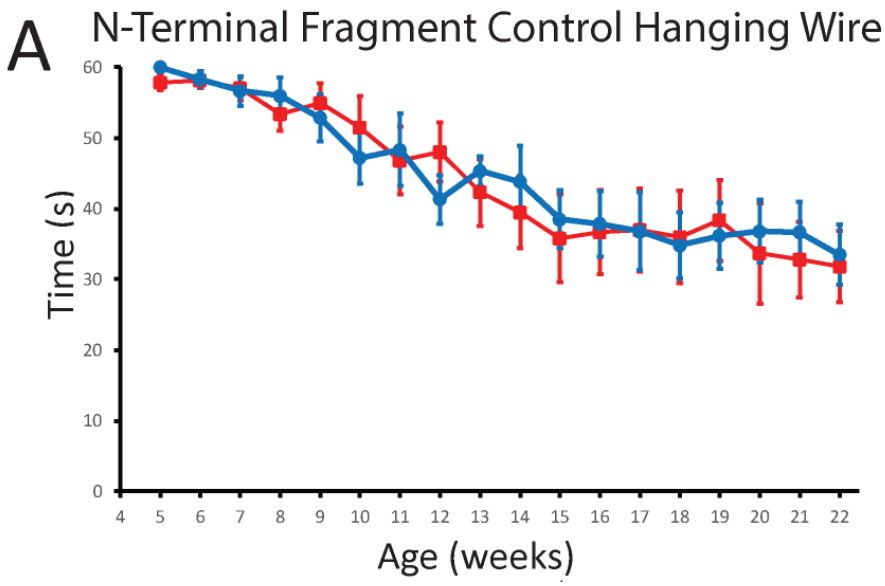

Figure 13 Legend: Hanging wire performance of mice administered AAV9 containing the N-terminal fragment of TDP-43 alone (NTF, blue line) showed no improvement over untreated littermates (red line).

References

References

Aartsma-Rus, A. (2017). FDA approval of nusinersen for spinal muscular atrophy makes 2016 the year of splice modulating oligonucleotides. *Nucleic Acid Therapeutics, 27*(2), 67. doi:10.1089/nat.2017.0665

Aktas, Y., Yemisci, M., Andrieux, K., Grsoy, R. N., Alonso, M. J., Fernandez-Megia, E., . . . Couvreur, P. (2005). Development and brain delivery of chitosan-PEG nanoparticles functionalized with the monoclonal antibody OX26. *Bioconjugate Chemistry, 16*(6), 1503.

Alami, N. H., Smith, R. B., Carrasco, M. A., Williams, L. A., Winborn, C. S., Han, S. S. W., . . . Taylor, J. P. (2014). Axonal transport of TDP-43 mRNA granules is impaired by ALS-causing mutations. *Neuron, 81*(3), 536. doi:10.1016/j.neuron.2013.12.018

Al-Chalabi, A., Andersen, P. M., Nilsson, P., Chioza, B., Andersson, J. L., Russ, C., . . . Leigh, P. N. (1999). Deletions of the heavy neurofilament subunit tail in amyotrophic lateral sclerosis. *Human Molecular Genetics, 8*(2), 157. Retrieved from http://search.ebscohost.com/login.aspx?direct=true&db=cmedm&AN=9931323&site=ehost-live&scope=site

Amador-Ortiz, C., Lin, W. L., Ahmed, Z., Personett, D., Davies, P., Duara, R., . . . Dickson, D. W. (2007). TDP-43 immunoreactivity in hippocampal sclerosis and alzheimer's disease. *Annals of Neurology, 61*(5), 435.

Arai, T., Hasegawa, M., Akiyama, H., Ikeda, K., Nonaka, T., Mori, H., . . . Oda, T. (2006a). TDP-43 is a component of ubiquitin-positive tau-negative inclusions in frontotemporal lobar

degeneration and amyotrophic lateral sclerosis. *Biochemical and Biophysical Research Communications, 351*(3), 602. Retrieved from http://search.ebscohost.com/login.aspx?direct=true&db=cmedm&AN=17084815&site=ehost-live&scope=site

Arai, T., Hasegawa, M., Akiyama, H., Ikeda, K., Nonaka, T., Mori, H., . . . Oda, T. (2006b). TDP-43 is a component of ubiquitin-positive tau-negative inclusions in frontotemporal lobar degeneration and amyotrophic lateral sclerosis. *Biochemical & Biophysical Research Communications, 351*(3), 602. doi:10.1016/j.bbrc.2006.10.093

Ash, P. E., Zhang, Y. J., Roberts, C. M., Saldi, T., Hutter, H., Buratti, E., . . . Link, C. D. (2010). Neurotoxic effects of TDP-43 overexpression in C. elegans. *Human Molecular Genetics, 19*(16), 3206. doi:10.1093/hmg/ddq230

Baumer, D., Hilton, D., Paine, S. M. L., Turner, M. R., Lowe, J., Talbot, K., & Ansorge, O. (2010). Juvenile ALS with basophilic inclusions is a FUS proteinopathy with FUS mutations. *Neurology, 75*(7), 611. doi:10.1212/WNL.0b013e3181ed9cde

Becker, L. A., Huang, B., Bieri, G., Ma, R., Knowles, D. A., Jafar-Nejad, P., . . . Gitler, A. D. (2017a). Therapeutic reduction of ataxin-2 extends lifespan and reduces pathology in TDP-43 mice. *Nature, 544*(7650), 367. doi:10.1038/nature22038

Becker, L. A., Huang, B., Bieri, G., Ma, R., Knowles, D. A., Jafar-Nejad, P., . . . Gitler, A. D. (2017b). Therapeutic reduction of ataxin-2 extends lifespan and reduces pathology in TDP-43 mice. *Nature, 544*(7650), 367. doi:10.1038/nature22038

Boylan, K. (2015). Familial amyotrophic lateral sclerosis. *Neurologic Clinics, 33*(4), 807. doi:10.1016/j.ncl.2015.07.001

Brady, O. A., Meng, P., Zheng, Y., Mao, Y., & Hu, F. (2011). Regulation of TDP-43 aggregation by phosphorylation and p62/SQSTM1. *Journal of Neurochemistry, 116*(2), 248. doi:10.1111/j.1471-4159.2010.07098.x

Buratti, E., Drk, T., Zuccato, E., Pagani, F., Romano, M., & Baralle, F. E. (2001). Nuclear factor TDP-43 and SR proteins promote in vitro and in vivo CFTR exon 9 skipping. *The EMBO Journal, 20*(7), 1774.

Burger, C., Gorbatyuk, O. S., Velardo, M. J., Peden, C. S., Williams, P., Zolotukhin, S., . . . Muzyczka, N. (2004). Recombinant AAV viral vectors pseudotyped with viral capsids from serotypes 1, 2, and 5 display differential efficiency and cell tropism after delivery to different regions of the central nervous. *Molecular Therapy: The Journal of the American Society of Gene Therapy, 10*(2), 302.

Cady, J., Koval, E. D., Benitez, B. A., Zaidman, C., Jockel-Balsarotti, J., Allred, P., . . . Harms, M. B. (2014). TREM2 variant p.R47H as a risk factor for sporadic amyotrophic lateral sclerosis. *JAMA Neurology, 71*(4), 449. doi:10.1001/jamaneurol.2013.6237

Cannon, J. R., Sew, T., Montero, L., Burton, E. A., & Greenamyre, J. T. (2011). Pseudotype-dependent lentiviral transduction of astrocytes or neurons in the rat substantia nigra. *Experimental Neurology, 228*(1), 41. doi:10.1016/j.expneurol.2010.10.016

Casafont, I., Bengoechea, R., Tapia, O., Berciano, M. T., & Lafarga, M. (2009). TDP-43 localizes in mRNA transcription and processing sites in mammalian neurons. *Journal of Structural Biology, 167*(3), 235. doi:10.1016/j.jsb.2009.06.006

Chakrabarty, P., Rosario, A., Cruz, P., Siemienski, Z., Ceballos-Diaz, C., Crosby, K., . . . Levites, Y. (2013). Capsid serotype and timing of injection determines AAV transduction in the neonatal mice brain. *PLoS ONE, 8*(6), 1. doi:10.1371/journal.pone.0067680

Chan, K. Y., Jang, M. J., Yoo, B. B., Greenbaum, A., Ravi, N., Wu, W. L., . . . Gradinaru, V. (2017). Engineered AAVs for efficient noninvasive gene delivery to the central and peripheral nervous systems. *Nature Neuroscience, 20*(8), 1172. doi:10.1038/nn.4593

Chew, J., Gendron, T. F., Prudencio, M., Sasaguri, H., Zhang, Y., Castanedes-Casey, M., . . . Petrucelli, L. (2015). C9ORF72 repeat expansions in mice cause TDP-43 pathology, neuronal loss, and behavioral deficits. *Science, 348*(6239), 1151.

Chiang, P. M., Ling, J., Jeong, Y. H., Price, D. L., Aja, S. M., & Wong, P. C. (2010). Deletion of TDP-43 down-regulates Tbc1d1, a gene linked to obesity, and alters body fat metabolism. *Proceedings of the National Academy of Sciences of the United States of America, 107*(37), 16320. doi:10.1073/pnas.1002176107

Chianga, P., Ling, J., Jeong, Y. H., Price, D. L., Aja, S. M., & Wong, P. C. (2010). Deletion of TDP-43 down-regulates Tbc1d1, a gene linked to obesity, and alters body fat metabolism. *PNAS Proceedings of the National Academy of Sciences of the United States of America, 107*(37), 16320. doi:10.1073/pnas.1002176107

Chou, C. C., Zhang, Y., Umoh, M. E., Vaughan, S. W., Lorenzini, I., Liu, F., . . . Rossoll, W. (2018). TDP-43 pathology disrupts nuclear pore complexes and nucleocytoplasmic transport in ALS/FTD. *Nature Neuroscience, 21*(2), 228. doi:10.1038/s41593-017-0047-3

Chow, C. Y., Landers, J. E., Bergren, S. K., Sapp, P. C., Grant, A. E., Jones, J. M., . . . Meisler, M. H. (2009). Deleterious variants of FIG4, a phosphoinositide phosphatase, in patients with ALS. *American Journal of Human Genetics, 84*(1), 85. doi:10.1016/j.ajhg.2008.12.010

Cirulli, E. T., Lasseigne, B. N., Petrovski, S., Sapp, P. C., Dion, P. A., Leblond, C. S., . . . Goldstein, D. B. (2015a). Exome sequencing in amyotrophic lateral sclerosis identifies risk genes and pathways. *Science (New York, N.Y.), 347*(6229), 1436. doi:10.1126/science.aaa3650

Cirulli, E. T., Lasseigne, B. N., Petrovski, S., Sapp, P. C., Dion, P. A., Leblond, C. S., . . . Goldstein, D. B. (2015b). Exome sequencing in amyotrophic lateral sclerosis identifies risk genes and pathways. *Science (New York, N.Y.), 347*(6229), 1436. doi:10.1126/science.aaa3650

Cleveland, D. W., Rothstein, J. D., Cleveland, D. W., & Rothstein, J. D. (2001). From charcot to lou gehrig: Deciphering selective motor neuron death in ALS. *Nature Reviews Neuroscience, 2*(11), 806. doi:10.1038/35097565

Cockrell, A. S., & Kafri, T. (2007). Gene delivery by lentivirus vectors. *Molecular Biotechnology, 36*(3), 184.

Conicella, A. E., Zerze, G. H., Mittal, J., & Fawzi, N. L. (2016). ALS mutations disrupt phase separation mediated by a-helical structure in the TDP-43 low-complexity C-terminal domain. *Structure, 24*(9), 1537. doi:10.1016/j.str.2016.07.007

Corey, D. R. (2017). Nusinersen, an antisense oligonucleotide drug for spinal muscular atrophy. *Nature Neuroscience, 20*(4), 497. doi:10.1038/nn.4508

Corrado, L., Carlomagno, Y., Falasco, L., Mellone, S., Godi, M., Cova, E., . . . D'Alfonso, S. (2011). A novel peripherin gene (PRPH) mutation identified in one sporadic amyotrophic lateral sclerosis patient. *Neurobiology of Aging, 32*(3), e1. doi:10.1016/j.neurobiolaging.2010.02.011

Cox, L. E., Ferraiuolo, L., Goodall, E. F., Heath, P. R., Higginbottom, A., Mortiboys, H., . . . Shaw, P. J. (2010). Mutations in CHMP2B in lower motor neuron predominant amyotrophic lateral sclerosis (ALS). *PLoS ONE, 5*(3), 1. doi:10.1371/journal.pone.0009872

Davtyan, H., Ghochikyan, A., Movsesyan, N., Ellefsen, B., Petrushina, I., Cribbs, D. H., . . . Agadjanyan, M. G. (2012). Delivery of a DNA vaccine for alzheimer's disease by electroporation versus gene gun generates potent and similar immune responses. *Neuro-Degenerative Diseases, 10*(1-4), 261. doi:10.1159/000333359

de Backer, M. W., Brans, M. A., Luijendijk, M. C., Garner, K. M., & Adan, R. A. (2010). Optimization of adeno-associated viral vector-mediated gene delivery to the hypothalamus. *Human Gene Therapy, 21*(6), 673. doi:10.1089/hum.2009.169

Deacon, R. M. (2013). Measuring motor coordination in mice. *Journal of Visualized Experiments: Jove,* (75), e2609. doi:10.3791/2609

del Aguila, M. A., Jr, L. W., McGuire, V., Koepsell, T. D., & van Belle, G. (2003). Prognosis in amyotrophic lateral sclerosis: A population-based study. *Neurology, 60*(5), 813. Retrieved from http://search.ebscohost.com/login.aspx?direct=true&db=rzh&AN=106887311&site=ehost-live&scope=site

DeVos, S. L., Goncharoff, D. K., Chen, G., Kebodeaux, C. S., Yamada, K., Stewart, F. R., . . . Miller, T. M. (2013). Antisense reduction of tau in adult mice protects against seizures. *The Journal of Neuroscience, 33*(31), 12887. doi:10.1523/JNEUROSCI.2107-13.2013

Donde, A., Wong, P. C., & Chen, L. L. (2017). Challenges and advances in gene therapy approaches for neurodegenerative disorders. *Current Gene Therapy, 17*(3), 187. doi:10.2174/1566523217666171013124150

Donnelly, C. J., Zhang, P. W., Pham, J. T., Haeusler, A. R., Mistry, N. A., Vidensky, S., . . . Rothstein, J. D. (2013). RNA toxicity from the ALS/FTD C9ORF72 expansion is mitigated by antisense intervention. *Neuron, 80*(2), 415. doi:10.1016/j.neuron.2013.10.015

Elden, A. C., Kim, H., Hart, M. P., Chen-Plotkin, A., Johnson, B. S., Fang, X., . . . Lee, V. M. -. (2010). Ataxin-2 intermediate-length polyglutamine expansions are associated with increased risk for ALS. *Nature, 466*(7310), 1069. doi:10.1038/nature09320

Evans, J. T., & Garcia, J. V. (2000). Lentivirus vector mobilization and spread by human immunodeficiency virus. *Human Gene Therapy, 11*(17), 2331.

Fecto, F., Yan, J., Vemula, S. P., Liu, E., Yang, Y., Chen, W., . . . Siddique, T. (2011). SQSTM1 mutations in familial and sporadic amyotrophic lateral sclerosis. *Archives of Neurology, 68*(11), 1440. doi:10.1001/archneurol.2011.250

Feiguin, F., Godena, V. K., Romano, G., D'Ambrogio, A., Klima, R., & Baralle, F. E. (2009). Depletion of TDP-43 affects drosophila motoneurons terminal synapsis and locomotive behavior. *FEBS Letters, 583*(10), 1586. doi:10.1016/j.febslet.2009.04.019

Fiesel, F. C., Voigt, A., Weber, S. S., Van den Haute, C., Waldenmaier, A., Grner, K., . . . Kahle, P. J. (2010). Knockdown of transactive response DNA-binding protein (TDP-43) downregulates histone deacetylase 6. *The EMBO Journal, 29*(1), 209. doi:10.1038/emboj.2009.324

Foust, K. D., Nurre, E., Montgomery, C. L., Hernandez, A., Chan, C. M., & Kaspar, B. K. (2009). Intravascular AAV9 preferentially targets neonatal neurons and adult astrocytes. *Nature Biotechnology, 27*(1), 59. doi:10.1038/nbt.1515

Foust, K. D., Wang, X., McGovern, V. L., Braun, L., Bevan, A. K., Haidet, A. M., . . . Kaspar, B. K. (2010). Rescue of the spinal muscular atrophy phenotype in a mouse model by early postnatal delivery of SMN. *Nature Biotechnology, 28*(3), 271. doi:10.1038/nbt.1610

Freibaum, B. D., Chitta, R. K., High, A. A., & Taylor, J. P. (2010). Global analysis of TDP-43 interacting proteins reveals strong association with RNA splicing and translation machinery. *Journal of Proteome Research, 9*(2), 1104. doi:10.1021/pr901076y

Freischmidt, A., Wieland, T., Richter, B., Ruf, W., Schaeffer, V., M﷿ller, K., . . . Nordstr﷿m, U. (2015). Haploinsufficiency of TBK1 causes familial ALS and fronto-temporal dementia. *Nature Neuroscience, 18*(5), 631. doi:10.1038/nn.4000

Gendron, T. F., Josephs, K. A., & Petrucelli, L. (2010). Review: Transactive response DNA-binding protein 43 (TDP-43): Mechanisms of neurodegeneration. *Neuropathology & Applied Neurobiology, 36*(2), 97. doi:10.1111/j.1365-2990.2009.01060.x

Gopal, P. P., Nirschl, J. J., Klinman, E., & Holzbaur, E. L. (2017). Amyotrophic lateral sclerosis-linked mutations increase the viscosity of liquid-like TDP-43 RNP granules in neurons. *Proceedings of the National Academy of Sciences of the United States of America, 114*(12), E2466. doi:10.1073/pnas.1614462114

Grattan-Smith, P., Hopkins, I. J., Shield, L. K., & Boldt, D. W. (1989). Acute pseudobulbar palsy due to bilateral focal cortical damage: The opercular syndrome of foix-chavany-marie. *Journal of Child Neurology, 4*(2), 131. Retrieved from http://search.ebscohost.com/login.aspx?direct=true&db=awn&AN=2715610&site=ehost-live&scope=site

Gromak, N., Rideau, A., Southby, J., Scadden, A. D., Gooding, C., Httelmaier, S., . . . Smith, C. W. (2003). The PTB interacting protein raver1 regulates alpha-tropomyosin alternative splicing. *The EMBO Journal, 22*(23), 6356.

Hanson, K. A., Kim, S. H., Wassarman, D. A., & Tibbetts, R. S. (2010). Ubiquilin modifies TDP-43 toxicity in a drosophila model of amyotrophic lateral sclerosis (ALS). *The Journal of Biological Chemistry, 285*(15), 11068. doi:10.1074/jbc.C109.078527

Hirano, M., Quinzii, C. M., Mitsumoto, H., Hays, A. P., Roberts, J. K., Richard, P., & Rowland, L. P. (2011). Senataxin mutations and amyotrophic lateral sclerosis. *Amyotrophic Lateral Sclerosis, 12*(3), 223. doi:10.3109/17482968.2010.545952

Howard, D. B., Powers, K., Wang, Y., & Harvey, B. K. (2008). Tropism and toxicity of adeno-associated viral vector serotypes 1, 2, 5, 6, 7, 8, and 9 in rat neurons and glia in vitro. *Virology, 372*(1), 24.

Iguchi, Y., Katsuno, M., Niwa, J., Takagi, S., Ishigaki, S., Ikenaka, K., . . . Sobue, G. (2013). Loss of TDP-43 causes age-dependent progressive motor neuron degeneration. *Brain: A Journal of Neurology, 136*(5), 1371. doi:10.1093/brain/awt029

Janson, C., McPhee, S., Bilaniuk, L., Haselgrove, J., Testaiuti, M., Freese, A., . . . Leone, P. (2002). Clinical protocol. gene therapy of canavan disease: AAV-2 vector for neurosurgical delivery of aspartoacylase gene (ASPA) to the human brain. *Human Gene Therapy, 13*(11), 1391.

Jeong, Y. H., Ling, J. P., Lin, S. Z., Donde, A. N., Braunstein, K. E., Majounie, E., . . . Wong, P. C. (2017). Tdp-43 cryptic exons are highly variable between cell types. *Molecular Neurodegeneration, 12*, 1. doi:10.1186/s13024-016-0144-x

Johnson, J. O., Mandrioli, J., Benatar, M., Abramzon, Y., Van Deerlin, V. M., Trojanowski, J. Q., . . . Traynor, B. J. (2010). Exome sequencing reveals VCP mutations as a cause of familial ALS. *Neuron, 68*(5), 857. doi:10.1016/j.neuron.2010.11.036

Johnson, J. O., Pioro, E. P., Boehringer, A., Chia, R., Feit, H., Renton, A. E., . . . Traynor, B. J. (2014). Mutations in the matrin 3 gene cause familial amyotrophic lateral sclerosis. *Nature Neuroscience, 17*(5), 664. doi:10.1038/nn.3688

Jones, C. T., Brock, D. J., Chancellor, A. M., Warlow, C. P., & Swingler, R. J. (1993). Cu/zn superoxide dismutase (SOD1) mutations and sporadic amyotrophic lateral sclerosis. *Lancet (London, England), 342*(8878), 1050. Retrieved from http://search.ebscohost.com/login.aspx?direct=true&db=cmedm&AN=8105280&site=ehost-live&scope=site

Josephs, K. A., Whitwell, J. L., Weigand, S. D., Murray, M. E., Tosakulwong, N., Liesinger, A. M., . . . Dickson, D. W. (2014). TDP-43 is a key player in the clinical features associated with alzheimer's disease. *Acta Neuropathologica, 127*(6), 811. doi:10.1007/s00401-014-1269-z

Julien, J. P. (2001). Amyotrophic lateral sclerosis. unfolding the toxicity of the misfolded. *Cell, 104*(4), 581. Retrieved from

http://search.ebscohost.com/login.aspx?direct=true&db=cmedm&AN=11239414&site=ehost-live&scope=site

Kabashi, E., Valdmanis, P. N., Dion, P., Spiegelman, D., McConkey, B. J., Vande Velde, C., . . . Rouleau, G. A. (2008). TARDBP mutations in individuals with sporadic and familial amyotrophic lateral sclerosis. *Nature Genetics, 40*(5), 572. doi:10.1038/ng.132

Kanekura, K., Nishimoto, I., Aiso, S., & Matsuoka, M. (2006). Characterization of amyotrophic lateral sclerosis-linked P56S mutation of vesicle-associated membrane protein-associated protein B (VAPB/ALS8). *The Journal of Biological Chemistry, 281*(40), 30223. Retrieved from http://search.ebscohost.com/login.aspx?direct=true&db=cmedm&AN=16891305&site=ehost-live&scope=site

Kaplitt, M. G., Leone, P., Samulski, R. J., Xiao, X., Pfaff, D. W., O'Malley, K. L., & During, M. J. (1994). Long-term gene expression and phenotypic correction using adeno-associated virus vectors in the mammalian brain. *Nature Genetics, 8*(2), 148-154.

Kawamoto, S., Shi, Q., Nitta, Y., Miyazaki, J., & Allen, M. D. (2005). Widespread and early myocardial gene expression by adeno-associated virus vector type 6 with a -actin hybrid promoter. *Molecular Therapy, 11*(6), 980. doi:10.1016/j.ymthe.2005.02.009

Kenna, K. P., van Doormaal, P. T., Dekker, A. M., Ticozzi, N., Kenna, B. J., Diekstra, F. P., . . . Landers, J. E. (2016). NEK1 variants confer susceptibility to amyotrophic lateral sclerosis. *Nature Genetics, 48*(9), 1037. doi:10.1038/ng.3626

Koltover, I., Salditt, T., Rdler, J. O., & Safinya, C. R. (1998). An inverted hexagonal phase of cationic liposome-DNA complexes related to DNA release and delivery. *Science (New York, N.Y.), 281*(5373), 78.

Kon, T., Mori, F., Tanji, K., Miki, Y., Toyoshima, Y., Yoshida, M., . . . Wakabayashi, K. (2014). ALS-associated protein FIG4 is localized in pick and lewy bodies, and also neuronal nuclear inclusions, in polyglutamine and intranuclear inclusion body diseases. *Neuropathology, 34*(1), 19. doi:10.1111/neup.12056

Konno, T., Ross, O. A., Teive, H. A. G., Slawek, J., Dickson, D. W., & Wszolek, Z. K. (2017). DCTN1-related neurodegeneration: Perry syndrome and beyond. *Parkinsonism & Related Disorders, 41*, 14. doi:10.1016/j.parkreldis.2017.06.004

Kraemer, B. C., Schuck, T., Wheeler, J. M., Robinson, L. C., Trojanowski, J. Q., Lee, V. M. Y., & Schellenberg, G. D. (2010). Loss of murine TDP-43 disrupts motor function and plays an essential role in embryogenesis. *Acta Neuropathologica, 119*(4), 409. doi:10.1007/s00401-010-0659-0

LaClair, K. D., Donde, A., Ling, J. P., Jeong, Y. H., Chhabra, R., Martin, L. J., & Wong, P. C. (2016). Depletion of TDP-43 decreases fibril and plaque -amyloid and exacerbates neurodegeneration in an alzheimers mouse model. *Acta Neuropathologica, 132*(6), 859. doi:10.1007/s00401-016-1637-y

Lambrechts, D., Storkebaum, E., Morimoto, M., Del-Favero, J., Desmet, F., Marklund, S. L., . . . Vermeire, S. (2003). VEGF is a modifier of amyotrophic lateral sclerosis in mice and humans

and protects motoneurons against ischemic death. *Nature Genetics, 34*(4), 383. doi:10.1038/ng1211

Lim, S. R., & Hertel, K. J. (2001). Modulation of survival motor neuron pre-mRNA splicing by inhibition of alternative 3' splice site pairing. *The Journal of Biological Chemistry, 276*(48), 45476.

Ling, J. P., Pletnikova, O., Troncoso, J. C., & Wong, P. C. (2015). TDP-43 repression of nonconserved cryptic exons is compromised in ALS-FTD. *Science (New York, N.Y.), 349*(6248), 650. doi:10.1126/science.aab0983

Lomen-Hoerth, C., Anderson, T., & Miller, B. (2002). The overlap of amyotrophic lateral sclerosis and frontotemporal dementia. *Neurology, 59*(7), 1077. Retrieved from http://search.ebscohost.com/login.aspx?direct=true&db=cmedm&AN=12370467&site=ehost-live&scope=site

Lorson, C. L., Hahnen, E., Androphy, E. J., & Wirth, B. (1999). A single nucleotide in the SMN gene regulates splicing and is responsible for spinal muscular atrophy. *Proceedings of the National Academy of Sciences of the United States of America, 96*(11), 6307.

Mackenzie, I. R., Bigio, E. H., Ince, P. G., Geser, F., Neumann, M., Cairns, N. J., . . . Trojanowski, J. Q. (2007). Pathological TDP-43 distinguishes sporadic amyotrophic lateral sclerosis from amyotrophic lateral sclerosis with SOD1 mutations. *Annals of Neurology, 61*(5), 427.

Mamot, C., Nguyen, J. B., Pourdehnad, M., Hadaczek, P., Saito, R., Bringas, J. R., . . . Bankiewicz, K. S. (2004). Extensive distribution of liposomes in rodent brains and brain tumors following convection-enhanced delivery. *Journal of Neuro-Oncology, 68*(1), 1.

McDonald, K. K., Aulas, A., Destroismaisons, L., Pickles, S., Beleac, E., Camu, W., . . . Vande Velde, C. (2011). TAR DNA-binding protein 43 (TDP-43) regulates stress granule dynamics via differential regulation of G3BP and TIA-1. *Human Molecular Genetics, 20*(7), 1400. doi:10.1093/hmg/ddr021

McLean, J. R., Smith, G. A., Rocha, E. M., Hayes, M. A., Beagan, J. A., Hallett, P. J., & Isacson, O. (2014). Widespread neuron-specific transgene expression in brain and spinal cord following synapsin promoter-driven AAV9 neonatal intracerebroventricular injection. *Neuroscience Letters, 576*, 73. doi:10.1016/j.neulet.2014.05.044

McMenamin, M. M., & Wood, M. J. A. (2010). Progress and prospects: Immunobiology of gene therapy for neurodegenerative disease: Prospects and risks. *Gene Therapy, 17*(4), 448. doi:10.1038/gt.2010.2

Mendell, J. R., Al-Zaidy, S., Shell, R., Arnold, W. D., Rodino-Klapac, L., Prior, T. W., . . . Braun, L. (2017). Single-dose gene-replacement therapy for spinal muscular atrophy. *New England Journal of Medicine, 377*(18), 1713. doi:10.1056/NEJMoa1706198

Miller, T. M., Pestronk, A., David, W., Rothstein, J., Simpson, E., Appel, S. H., . . . Cudkowicz, M. E. (2013). An antisense oligonucleotide against SOD1 delivered intrathecally for patients with SOD1 familial amyotrophic lateral sclerosis: A phase 1, randomised, first-in-man study.

The Lancet Neurology, 12(5), 435-442. doi://doi-org.proxy1.library.jhu.edu/10.1016/S1474-4422(13)70061-9

Molliex, A., Temirov, J., Lee, J., Coughlin, M., Kanagaraj, A. P., Kim, H. J., . . . Taylor, J. P. (2015). Phase separation by low complexity domains promotes stress granule assembly and drives pathological fibrillization. *Cell, 163*(1), 123. doi:10.1016/j.cell.2015.09.015

Naldini, L., Blmer, U., Gage, F. H., Trono, D., & Verma, I. M. (1996). Efficient transfer, integration, and sustained long-term expression of the transgene in adult rat brains injected with a lentiviral vector. *Proceedings of the National Academy of Sciences of the United States of America, 93*(21), 11382.

Neumann, M., Mackenzie, I. R., Cairns, N. J., Boyer, P. J., Markesbery, W. R., Smith, C. D., . . . Forman, M. S. (2007). TDP-43 in the ubiquitin pathology of frontotemporal dementia with VCP gene mutations. *Journal of Neuropathology and Experimental Neurology, 66*(2), 152. Retrieved from http://search.ebscohost.com/login.aspx?direct=true&db=cmedm&AN=17279000&site=ehost-live&scope=site

Neumann, M., Sampathu, D. M., Kwong, L. K., Truax, A. C., Micsenyi, M. C., Chou, T. T., . . . Lee, V. M. (2006). Ubiquitinated TDP-43 in frontotemporal lobar degeneration and amyotrophic lateral sclerosis. *Science (New York, N.Y.), 314*(5796), 130.

Ou, S. H., Wu, F., Harrich, D., Garca-Martnez, L. F., & Gaynor, R. B. (1995). Cloning and characterization of a novel cellular protein, TDP-43, that binds to human immunodeficiency virus type 1 TAR DNA sequence motifs. *Journal of Virology, 69*(6), 3584.

Pack, D. W., Hoffman, A. S., Pun, S., & Stayton, P. S. (2005). Design and development of polymers for gene delivery. *Nature Reviews Drug Discovery, 4*(7), 581-593. doi:10.1038/nrd1775

Parkinson, N., Ince, P. G., Smith, M. O., Highley, R., Skibinski, G., Andersen, P. M., . . . Pall, H. S. (2006). ALS phenotypes with mutations in CHMP2B (charged multivesicular body protein 2B). *Neurology, 67*(6), 1074. Retrieved from http://search.ebscohost.com/login.aspx?direct=true&db=rzh&AN=106149617&site=ehost-live&scope=site

Passini, M. A., Bu, J., Richards, A. M., Kinnecom, C., Sardi, S. P., Stanek, L. M., . . . Cheng, S. H. (2011). Antisense oligonucleotides delivered to the mouse CNS ameliorate symptoms of severe spinal muscular atrophy. *Science Translational Medicine, 3*(72), 72ra18. doi:10.1126/scitranslmed.3001777

Passini, M. A., & Wolfe, J. H. (2001). Widespread gene delivery and structure-specific patterns of expression in the brain after intraventricular injections of neonatal mice with an adeno-associated virus vector. *Journal of Virology, 75*(24), 12382.

Paubel, A., Violette, J., Amy, M., Praline, J., Meininger, V., Camu, W., . . . Vourc'h, P. (2008). Mutations of the ANG gene in french patients with sporadic amyotrophic lateral sclerosis. *Archives of Neurology, 65*(10), 1333. doi:10.1001/archneur.65.10.1333

Petrov, D., Mansfield, C., Moussy, A., & Hermine, O. (2017). ALS clinical trials review: 20 years of failure. are we any closer to registering a new treatment? *Frontiers in Aging Neuroscience, 9* Retrieved from http://search.ebscohost.com/login.aspx?direct=true&db=psyh&AN=2017-13499-001&site=ehost-live&scope=site

Polymenidou, M., Lagier-Tourenne, C., Hutt, K. R., Huelga, S. C., Moran, J., Liang, T. Y., . . . Cleveland, D. W. (2011). Long pre-mRNA depletion and RNA missplicing contribute to neuronal vulnerability from loss of TDP-43. *Nature Neuroscience, 14*(4), 459. doi:10.1038/nn.2779

Pringle, C. E., Hudson, A. J., Munoz, D. G., Kiernan, J. A., Brown, W. F., & Ebers, G. C. (1992). Primary lateral sclerosis. clinical features, neuropathology and diagnostic criteria. *Brain: A Journal of Neurology, 115 (Pt 2)*, 495. Retrieved from http://search.ebscohost.com/login.aspx?direct=true&db=cmedm&AN=1606479&site=ehost-live&scope=site

Prudencio, M., Belzil, V. V., Batra, R., Ross, C. A., Gendron, T. F., Pregent, L. J., . . . Rademakers, R. (2015). Distinct brain transcriptome profiles in C9orf72-associated and sporadic ALS. *Nature Neuroscience, 18*(8), 1175. doi:10.1038/nn.4065

Renton, A. E., Majounie, E., Waite, A., Sim﷽n-S﷽nchez, J., Rollinson, S., Gibbs, J. R., . . . Traynor, B. J. (2011). A hexanucleotide repeat expansion in C9ORF72 is the cause of chromosome 9p21-linked ALS-FTD. *Neuron, 72*(2), 257. doi:10.1016/j.neuron.2011.09.010

Rideau, A. P., Gooding, C., Simpson, P. J., Monie, T. P., Lorenz, M., Httelmaier, S., . . . Smith, C. W. J. (2006). A peptide motif in Raver1 mediates splicing repression by interaction with the PTB RRM2 domain. *Nature Structural & Molecular Biology, 13*(9), 839. doi:10.1038/nsmb1137

Rosen, D. R., Siddique, T., Patterson, D., Figlewicz, D. A., Sapp, P., Hentati, A., . . . Deng, H. X. (1993). Mutations in cu/zn superoxide dismutase gene are associated with familial amyotrophic lateral sclerosis. *Nature, 362*(6415), 59. Retrieved from http://search.ebscohost.com/login.aspx?direct=true&db=cmedm&AN=8446170&site=ehost-live&scope=site

Rossi, J., Balthasar, N., Olson, D., Scott, M., Berglund, E., Lee, C. E., . . . Elmquist, J. K. (2011). Melanocortin-4 receptors expressed by cholinergic neurons regulate energy balance and glucose homeostasis. *Cell Metabolism, 13*(2), 195. doi:10.1016/j.cmet.2011.01.010

Rutherford, N. J., Yong-Jie Zhang, Baker, M., Gass, J. M., Finch, N. A., Ya-Fei Xu, . . . Cashman, N. R. (2008). Novel mutations in TARDBP (TDP-43) in patients with familial amyotrophic lateral sclerosis. *PLoS Genetics, 4*(9), 1. doi:10.1371/journal.pgen.1000193

Salajegheh, M., Pinkus, J. L., Taylor, J. P., Amato, A. A., Nazareno, R., Baloh, R. H., . . . Greenberg, S. A. (2009). Sarcoplasmic redistribution of nuclear TDP-43 in inclusion body myositis. *Muscle & Nerve, 40*(1), 19. doi:10.1002/mus.21386

Sch�le, R., Wiethoff, S., Martus, P., Karle, K. N., Otto, S., Klebe, S., . . . Sch�ls, L. (2016). Hereditary spastic paraplegia: Clinicogenetic lessons from 608 patients. *Annals of Neurology, 79*(4), 646. doi:10.1002/ana.24611

Schmid, B., Hruscha, A., Hogl, S., Banzhaf-Strathmann, J., Strecker, K., van, d. Z., . . . Haass, C. (2013). Loss of ALS-associated TDP-43 in zebrafish causes muscle degeneration, vascular dysfunction, and reduced motor neuron axon outgrowth. *PNAS Proceedings of the National Academy of Sciences of the United States of America, 110*(13), 4986. doi:10.1073/pnas.1218311110

Sephton, C. F., Good, S. K., Atkin, S., Dewey, C. M., Mayer, P.,3rd, Herz, J., & Yu, G. (2010). TDP-43 is a developmentally regulated protein essential for early embryonic development. *The Journal of Biological Chemistry, 285*(9), 6826. doi:10.1074/jbc.M109.061846

Shan, X., Chiang, P. M., Price, D. L., & Wong, P. C. (2010). Altered distributions of gemini of coiled bodies and mitochondria in motor neurons of TDP-43 transgenic mice. *Proceedings of the National Academy of Sciences of the United States of America, 107*(37), 16325. doi:10.1073/pnas.1003459107

Shantanu, S., Vijayalakshmi, K., Shruthi, S., Sagar, B. K. C., Sathyaprabha, T. N., Nalini, A., . . . Alladi, P. A. (2017). VEGF alleviates ALS-CSF induced cytoplasmic accumulations of TDP-43 and FUS/TLS in NSC-34 cells. *Journal of Chemical Neuroanatomy, 81*, 48. doi:10.1016/j.jchemneu.2017.01.007

Shyam, R., Ren, Y., Lee, J., Braunstein, K. E., Mao, H. Q., & Wong, P. C. (2015). Intraventricular delivery of siRNA nanoparticles to the central nervous system. *Molecular Therapy.Nucleic Acids, 4*, e242. doi:10.1038/mtna.2015.15

Sieben, A., Van Langenhove, T., Engelborghs, S., Martin, J. J., Boon, P., Cras, P., . . . Cruts, M. (2012). The genetics and neuropathology of frontotemporal lobar degeneration. *Acta Neuropathologica, 124*(3), 353. doi:10.1007/s00401-012-1029-x

Smith, B. N., Ticozzi, N., Fallini, C., Gkazi, A. S., Topp, S., Kenna, K. P., . . . Landers, J. E. (2014). Exome-wide rare variant analysis identifies TUBA4A mutations associated with familial ALS. *Neuron, 84*(2), 324. doi:10.1016/j.neuron.2014.09.027

Smith, B. N., Topp, S. D., Fallini, C., Shibata, H., Chen, H. J., Troakes, C., . . . Shaw, C. E. (2017). Mutations in the vesicular trafficking protein annexin A11 are associated with amyotrophic lateral sclerosis. *Science Translational Medicine, 9*(388) doi:10.1126/scitranslmed.aad9157

Spiller, K. J., Cheung, C. J., Restrepo, C. R., Kwong, L. K., Stieber, A. M., Trojanowski, J. Q., & Lee, V. M. -. (2016). Selective motor neuron resistance and recovery in a new inducible mouse model of TDP-43 proteinopathy. *The Journal of Neuroscience, 36*(29), 7707. doi:10.1523/JNEUROSCI.1457-16.2016

Sreedharan, J., Blair, I. P., Tripathi, V. B., Hu, X., Vance, C., Rogelj, B., . . . Shaw, C. E. (2008). TDP-43 mutations in familial and sporadic amyotrophic lateral sclerosis. *Science (New York, N.Y.), 319*(5870), 1668. doi:10.1126/science.1154584

Sun, M., Bell, W., LaClair, K. D., Ling, J. P., Han, H., Kageyama, Y., . . . Chen, L. L. (2017a). Cryptic exon incorporation occurs in alzheimers brain lacking TDP-43 inclusion but exhibiting nuclear clearance of TDP-43. *Acta Neuropathologica, 133*(6), 923. doi:10.1007/s00401-017-1701-2

Sun, M., Bell, W., LaClair, K. D., Ling, J. P., Han, H., Kageyama, Y., . . . Chen, L. L. (2017b). Cryptic exon incorporation occurs in alzheimers brain lacking TDP-43 inclusion but exhibiting nuclear clearance of TDP-43. *Acta Neuropathologica, 133*(6), 923. doi:10.1007/s00401-017-1701-2

Swain, G. P., Prociuk, M., Bagel, J. H., O'Donnell, P., Berger, K., Drobatz, K., . . . Vite, C. H. (2014). Adeno-associated virus serotypes 9 and rh10 mediate strong neuronal transduction of the dog brain. *Gene Therapy, 21*(1), 28-36. doi:10.1038/gt.2013.54

Swash, M., & Desai, J. (2000). Motor neuron disease: Classification and nomenclature. *Amyotrophic Lateral Sclerosis & Other Motor Neuron Disorders, 1*(2), 105. Retrieved from http://search.ebscohost.com/login.aspx?direct=true&db=a9h&AN=4801988&site=ehost-live&scope=site

Tanaka, Y., & Hasegawa, M. (2016). Profilin 1 mutants form aggregates that induce accumulation of prion-like TDP-43. *Prion, 10*(4), 283. doi:10.1080/19336896.2016.1207033

Tanguy, Y., Biferi, M. G., Besse, A., Astord, S., Cohen-Tannoudji, M., Marais, T., & Barkats, M. (2015). Systemic AAVrh10 provides higher transgene expression than AAV9 in the brain and the spinal cord of neonatal mice. *Frontiers in Molecular Neuroscience, 8*, 36. doi:10.3389/fnmol.2015.00036

Taniguchi, Y., Young-Pearse, T., Sawa, A., & Kamiya, A. (2012). In utero electroporation as a tool for genetic manipulation in vivo to study psychiatric disorders: From genes to circuits and behaviors. *The Neuroscientist, 18*(2), 169. doi:10.1177/1073858411399925

Taylor, J. P., Brown, R.,Jr, & Cleveland, D. W. (2016). Decoding ALS: From genes to mechanism. *Nature, 539*(7628), 197. doi:10.1038/nature20413

Tollervey, J. R., Curk, T., Rogelj, B., Briese, M., Cereda, M., Kayikci, M., . . . Ule, J. (2011). Characterizing the RNA targets and position-dependent splicing regulation by TDP-43. *Nature Neuroscience, 14*(4), 452. doi:10.1038/nn.2778

Urwin, H., Josephs, K. A., Rohrer, J. D., Mackenzie, I. R., Neumann, M., Authier, A., . . . Isaacs, A. M. (2010). FUS pathology defines the majority of tau- and TDP-43-negative frontotemporal lobar degeneration. *Acta Neuropathologica, 120*(1), 33. doi:10.1007/s00401-010-0698-6

van Rheenen, W., Shatunov, A., Dekker, A. M., McLaughlin, R. L., Diekstra, F. P., Pulit, S. L., . . . Veldink, J. H. (2016). Genome-wide association analyses identify new risk variants and the genetic architecture of amyotrophic lateral sclerosis. *Nature Genetics, 48*(9), 1043. doi:10.1038/ng.3622

Vance, C., Rogelj, B., Hortobgyi, T., De Vos, K. J., Nishimura, A. L., Sreedharan, J., . . . Shaw, C. E. (2009). Mutations in FUS, an RNA processing protein, cause familial amyotrophic lateral sclerosis type 6. *Science (New York, N.Y.), 323*(5918), 1208. doi:10.1126/science.1165942

Vanden Broeck, L., Callaerts, P., & Dermaut, B. (2014). TDP-43-mediated neurodegeneration: Towards a loss-of-function hypothesis? *Trends in Molecular Medicine, 20*(2), 66. doi:10.1016/j.molmed.2013.11.003

Vatsavayai, S. C., Soo, J. Y., Gardner, R. C., Gendron, T. F., Vargas, J. N. S., Trujillo, A., . . . Yoon, S. J. (2016a). Timing and significance of pathological features in C9orf72 expansion-associated frontotemporal dementia. *Brain: A Journal of Neurology, 139*(12), 3202. doi:10.1093/brain/aww250

Vatsavayai, S. C., Soo, J. Y., Gardner, R. C., Gendron, T. F., Vargas, J. N. S., Trujillo, A., . . . Yoon, S. J. (2016b). Timing and significance of pathological features in C9orf72 expansion-associated frontotemporal dementia. *Brain: A Journal of Neurology, 139*(12), 3202. doi:10.1093/brain/aww250

Wais, V., Rosenbohm, A., Petri, S., Kollewe, K., Hermann, A., Storch, A., . . . Dorst, J. (2017). The concept and diagnostic criteria of primary lateral sclerosis. *Acta Neurologica Scandinavica, 136*(3), 204. doi:10.1111/ane.12713

Weinberg, M. S., Samulski, R. J., & McCown, T. J. (2013). Adeno-associated virus (AAV) gene therapy for neurological disease. *Neuropharmacology, 69*, 82-88. doi://doi.org/10.1016/j.neuropharm.2012.03.004

Williams, K. L., Topp, S., Yang, S., Smith, B., Fifita, J. A., Warraich, S. T., . . . Blair, I. P. (2016). CCNF mutations in amyotrophic lateral sclerosis and frontotemporal dementia. *Nature Communications, 7*, 11253. doi:10.1038/ncomms11253

Wils, H., Kleinberger, G., Janssens, J., Pereson, S., Joris, G., Cuijt, I., . . . Kumar-Singh, S. (2010). TDP-43 transgenic mice develop spastic paralysis and neuronal inclusions characteristic of ALS and frontotemporal lobar degeneration. *Proceedings of the National Academy of Sciences of the United States of America, 107*(8), 3858. doi:10.1073/pnas.0912417107

Winton, M. J., Igaz, L. M., Wong, M. M., Kwong, L. K., Trojanowski, J. Q., & Lee, V. M. (2008). Disturbance of nuclear and cytoplasmic TAR DNA-binding protein (TDP-43) induces disease-like redistribution, sequestration, and aggregate formation. *The Journal of Biological Chemistry, 283*(19), 13302. doi:10.1074/jbc.M800342200

Wu, C., Fallini, C., Ticozzi, N., Keagle, P. J., Sapp, P. C., Piotrowska, K., . . . Moore, M. J. (2012). Mutations in the profilin 1 gene cause familial amyotrophic lateral sclerosis. *Nature, 488*(7412), 499. doi:10.1038/nature11280

Wu, L. S., Cheng, W. C., Hou, S. C., Yan, Y. T., Jiang, S. T., & Shen, C. K. (2010). TDP-43, a neuro-pathosignature factor, is essential for early mouse embryogenesis. *Genesis (New York, N.Y.: 2000), 48*(1), 56. doi:10.1002/dvg.20584

Wu, L. S., Cheng, W. C., & Shen, C. K. (2012). Targeted depletion of TDP-43 expression in the spinal cord motor neurons leads to the development of amyotrophic lateral sclerosis-like

phenotypes in mice. *The Journal of Biological Chemistry, 287*(33), 27335. doi:10.1074/jbc.M112.359000

Xu, Y., Gendron, T. F., Zhang, Y., Lin, W., D'Alton, S., Sheng, H., . . . Petrucelli, L. (2010). Wild-type human TDP-43 expression causes TDP-43 phosphorylation, mitochondrial aggregation, motor deficits, and early mortality in transgenic mice. *The Journal of Neuroscience, 30*(32), 10851. doi:10.1523/JNEUROSCI.1630-10.2010

Yamashita, S., Kimura, E., Tawara, N., Sakaguchi, H., Nakama, T., Maeda, Y., . . . Ando, Y. (2013). Optineurin is potentially associated with TDP-43 and involved in the pathogenesis of inclusion body myositis. *Neuropathology & Applied Neurobiology, 39*(4), 406. doi:10.1111/j.1365-2990.2012.01297.x

Yang, C., Wang, H., Qiao, T., Yang, B., Aliaga, L., Qiu, L., . . . Xu, Z. (2014a). Partial loss of TDP-43 function causes phenotypes of amyotrophic lateral sclerosis. *Proceedings of the National Academy of Sciences of the United States of America, 111*(12), E1121. doi:10.1073/pnas.1322641111

Yang, C., Wang, H., Qiao, T., Yang, B., Aliaga, L., Qiu, L., . . . Xu, Z. (2014b). Partial loss of TDP-43 function causes phenotypes of amyotrophic lateral sclerosis. *Proceedings of the National Academy of Sciences of the United States of America, 111*(12), E1121. doi:10.1073/pnas.1322641111

Yang, Y., Hentati, A., Deng, H., Dabbagh, O., Sasaki, T., Hirano, M., . . . Siddique, T. (2001). The gene encoding alsin, a protein with three guanine-nucleotide exchange factor domains, is

mutated in a form of recessive amyotrophic lateral sclerosis. *Nature Genetics, 29*(2), 160. Retrieved from http://search.ebscohost.com/login.aspx?direct=true&db=a9h&AN=8781829&site=ehost-live&scope=site

Zhang, H., Yang, B., Mu, X., Ahmed, S. S., Su, Q., He, R., . . . Gao, G. (2011). Several rAAV vectors efficiently cross the blood-brain barrier and transduce neurons and astrocytes in the neonatal mouse central nervous system. *Molecular Therapy: The Journal of the American Society of Gene Therapy, 19*(8), 1440. doi:10.1038/mt.2011.98

Zhang, K., Donnelly, C. J., Haeusler, A. R., Grima, J. C., Machamer, J. B., Steinwald, P., . . . Lloyd, T. E. (2015). The C9orf72 repeat expansion disrupts nucleocytoplasmic transport. *Nature, 525*(7567), 56. doi:10.1038/nature14973

Zuo-Shang Xu. (2012). Does a loss of TDP-43 function cause neurodegeneration? *Molecular Neurodegeneration, 7*(1), 27. doi:10.1186/1750-1326-7-27

Aneesh Nitin Donde

929 N. Wolfe Street 516A ▪ Baltimore, MD 21205 ▪ (408) 821-9202 ▪ aneeshdonde@gmail.com ▪ adonde1@jhu.edu

---

EDUCATION

JOHNS HOPKINS UNIVERSITY 2012-2018
PhD Neuroscience

UNIVERSITY OF CALIFORNIA-BERKELEY 2007-2011
B.A. Molecular & Cellular Biology - Neurobiology GPA: 3.81

RESEARCH EXPERIENCE

Philip C. Wong Lab Johns Hopkins, 2012-2018
PhD Thesis Project

- Investigated the link between Tar DNA-binding protein 43 (TDP-43) dysfunction and pathogenesis of amyotrophic lateral sclerosis (ALS).
- Characterized behavioral and pathological deficits of multiple tissue-specific TDP-43 conditional knockout mice.
- Demonstrated that splicing repression is a major function of TDP-43 in neurons using a multi-organism approach.
- Validated a novel mechanism-based gene therapy treatment strategy for ALS.

William Jagust Lab UC Berkeley, 2010-2012

- Undergraduate honors thesis on the effects of striatal dopamine on cognitive flexibility through analysis of human fMRI and PET scans.

Mehrdad Arjomandi Lab UC San Francisco, 2008-2011

- Research apprenticeship at the UCSF Lung Biology Center exploring the molecular underpinnings of airway inflammation in rodent models and human subjects.

HONORS

Oustanding Abstract in Basic Research Johns Hopkins, 2015 & 2017
Pathology Young Investigators' Symposium

National Science Foundation GFRP Honorable Mention — Johns Hopkins, 2013 & 2014

I.L Chaikoff Memorial Award — UC Berkeley, 2011

B.A with Academic Honors — UC Berkeley, 2011

PUBLICATIONS

Donde A, Ling J, Braunstein K, Sun M, Chen L, Jeong YH, Pang B, Wen X, Wong P. Splicing Repression is a Major Function of TDP-43 in Neurons: Identification of a Novel Therapeutic Target for ALS/FTD. (In prepraration).

Donde A, Chen L, Wong P. Challenges and Advances in Gene Therapy Approaches for Neurodegenerative Disorders. Curr. Gene Ther. 2017 Oct 13;

LaClair K, **Donde A**, Ling J, Jeong YH, Chhabra R, Martin L, Wong P. Depletion of TDP-43 decreases fibril and plaque β-amyloid and exacerbates neurodegeneration in an Alzheimer's mouse model. Acta Neuropathol. 2016 Dec;132(6):859-873.

Jeong YH, Ling J, Lin S, **Donde A**, Braunstein K, Majounie E, Traynor B, LaClair K, Lloyd T, Wong P . Tdp-43 cryptic exons are highly variable between cell types. Molecular Neurodegeneration. 2017;12:1.

Holland, N, Davé, V, Venkat, S, Wong, H, **Donde, A**, Balmes, J, Arjomandi, M. (2015), Ozone inhalation leads to a dose-dependent increase of cytogenetic damage in human lymphocytes. Environ. Mol. Mutagen., 56: 378–387. doi:10.1002/em.21921

Arjomandi M, Wong H, **Donde A**, Frelinger J, Dalton S, Ching W, Power K, Balmes J. Exposure to medium and high ambient levels of ozone causes adverse systemic inflammatory and cardiac autonomic effects. Am J Physiol Heart Circ Physiol. 2015 Jun 15;308(12):H1499-509. doi: 10.1152/ajpheart.00849.2014.

Donde A, Wong H, Frelinger J, Power K, Balmes J, Arjomandi M. Effects of Exercise on Systemic Inflammatory, Coagulatory, and Cardiac Autonomic Parameters in an Inhalational Exposure Study. J Occup Environ Med. 2012 April ;54(4):466-70

Dang L*, **Donde A***, Madison C, O'Neil J, Jagust, W. 2012. Striatal dopamine influences the default mode network to affect shifting between object features. J. Cognitive Neuroscience 2012 Sep, 1960-1970. *co-1st authors

Arjomandi M, Frelinger J, **Donde A**, Wong H, Yellamilli A, Raymond W. Secreted Osteopontin Is Highly Polymerized in Human Airways and Fragmented in Asthmatic Airway Secretions. PLoS ONE 2011 6(10): e25678. doi:10.1371/journal.pone.00256

CONFERENCES/PRESENTATIONS

- *Society for Neuroscience, Washington DC:* Splicing Repression is a Major Function of TDP-43 in Motor Neurons: Identification of a Therapeutic Target for ALS/FTD. Donde, A., Ling, J., Braunstein, K., Cheng, X., Wong, P. 2017
- *Gordon Research Conference, Stoweflake, VT*: Splicing Repression is a Major Function of TDP-43 in Motor Neurons: Identification of a Therapeutic Target for ALS/FTD. Donde, A., Ling, J., Braunstein, K., Cheng, X., Wong, P. 2017
- *Pathology Young Investigators' Symposium, Baltimore MD*: Splicing Repression is a Major Function of TDP-43 in Motor Neurons: Identification of a Therapeutic Target for ALS/FTD. Donde, A., Ling, J., Braunstein, K., Cheng, X., Wong, P. 2017
- *Pathology Young Investigators' Symposium, Baltimore MD*: Deletion of Neuronal Tdp-43 in ALS-FTD Models Promotes Neurodegeneration by Imparing Autophagy. Donde, A., Jeong, YH., Ling, J., Braunstein, K., Chen, L., Wong, P. 2015

TEACHING EXPERIENCE

Neuroscience and Cognition II — Johns Hopkins, 2013
Teaching Assistant